formed compact colonies typical of undifferentiated ES cells (Fig. 3A, panel d). Moreover, the upregulation of neural marker genes was inhibited (Fig. 3C). However, at 20 and 50 μM, U0126 appeared to be toxic, since we observed many vesicles emerging inside the cell and a dramatic increase in cell death (Fig. 3A, panels e and f). We then passaged U0126-treated and nontreated cells and cultured them in hESF9A for 7 days. Immunostaining was carried out to further examine the expression of OCT4, SIX3, and PAX6. We found that without prior U0126 treatment, cells formed "rosette-like" clusters and the expression of OCT4 protein was markedly reduced (Fig. 3C, panel a), while in the same cultures many rosette cells formed showing SIX3 and PAX6 nuclear staining (Fig. 3C, panels b and c). By contrast, after U0126 treatment, HUES1 cells did not form rosettes and maintained uniform nuclear OCT4 staining (Fig. 3C, panel d), while SIX3 and PAX6 proteins were not detected (Fig. 3C, panels e and f). U0126 also prevented neural differentiation from SHEF5 cells (Supplementary Figs. 2C and D).

ERK1/2 activation is required to counterbalance BMP-induced differentiation in monolayer culture

Human ES cells express several BMP ligands (Sperger et al., 2003). Moreover, the Knockout serum replacement in the conventional human ES cell culture medium includes BMP-like activities (Xu et al., 2005). Thus, we next tested whether ERK1/2 activation can counteract BMP-induced differentiation in human ES cells using the hESF-based monolayer culture system. After exposure to BMP4 for 5 days, human ES cell colonies lost their compact morphology, appearing flattened (Fig. 4A, panel a), and also lost the expression of the OCT4 protein (Fig. 4B, panel a). By contrast, when cells were cultured in the presence of 50 ng/ml of FGF2 together with BMP4, they maintained an undifferentiated morphology as well as nuclear OCT4 expression (Figs. 4A and B, panel c). Thus, FGF2 signaling appears to counteract the BMP pathway. However, when U0126 was added to BMP4 in the absence of FGF2, these flat cells appeared even earlier and more extensively than with BMP4 alone (Fig. 4A, panel b). We could not detect any OCT4 protein in these cells (Fig. 4B, panel b). U0126 treatment also almost abolished the ability of FGF2 to rescue the cells from BMP4-induced differentiation, as many flat cells were observed under the BMP4+FGF2 U0126 condition and OCT4 staining was absent in most of them (Figs. 4A and B, panel d). In agreement with the morphological changes, the RNA levels of the early extraembryonic lineage marker AFP increased markedly in BMP4-treated cells, but were downregulated when high concentrations of FGF2 were added (Supplementary Fig. 3). Cells cultured in the presence of BMP4, FGF, and U0126 showed similar upregulation of AFP as those treated with BMP4 alone (Supplementary Fig. 3). This suggests that one major role of FGF2–ERK1/2 signaling is to suppress the differentiation induced by BMP, which may explain the reports that ERK1/2 inhibition promotes the differentiation of human ES cells cultured in media containing KSR (Xu et al., 2002; Li et al., 2007).

ERK1/2 function is required for the attachment of human ES cells at low cell density

In the presence of U0126, we observed a reduction in the attachment of the human ES cells to the collagen substrate after passaging, resulting in a high proportion of cells floating in the media. To test the effect of U0126 on cell attachment more easily, we used a culture-adapted HUES1 subline that carried an extra chromosome 12p, because these cells survive better after trypsin dissociation into single cells. In condition A, HUES1 cells cultured in hESF9A without U0126 were dissociated into single cells and plated at 2000 cells/cm^2 density in hESF9A without U0126. In condition B, HUES1 cells were first cultured with U0126 for 5 days; the drug was then removed 2 h before harvesting and the cells were plated at the same density in hESF9A without U0126. In condition C, the cells were cultured without U0126 but plated in hESF9A containing U0126. The day after seeding, we found similar numbers of cells attached to the substrate in conditions A and B, whereas almost no cells attached in condition C (Figs. 5A and B). Thus, ERK1/2 activity appears to be required for cell adhesion and subsequent survival under single-cell or low-density conditions. After culturing the cells for 5 days after seeding in hESF9A, we added U0126 back into the condition B group and maintained the cultures for a further 5 days. A high-content screen was carried out to analyse the growth and differentiation status of the cells (Figs. 5C and D). On average, cultures maintained under conditions A and B had similar numbers of colonies and numbers of cells per field imaged, indicating that once cells are attached and have reached a certain density, U0126 does not affect their growth significantly. However, there were markedly more OCT4- and SSEA4-positive cells per field in condition B (when cells were cultured at later stages in U0126) than in condition A, suggesting that inhibition of ERK1/2 by U0126 reduced spontaneous differentiation (Fig. 5D, panels a and b). Under condition C, when cells were seeded in U0126 but cultured without it, there were very few colonies and only a small proportion of cells expressed OCT4 and SSEA4 (Fig. 5C, panel c, and D condition C). We also tested the effect of U0126 on karyotypically normal SHEF6 cells. Similar to HUES1, U0126 significantly reduced the number of single cells attached to the substrate and, consequently, almost no colony formed in this group (Supplementary Fig. 4). Taken together, these results indicate that ERK1/2 inhibition has a negative impact on cell attachment to the substrate.

Figure 2 (A) Morphology of HUES1 ES cells cultured in activin A (100 ng/ml) plus FGF2 (10 ng/ml) treated with increasing concentrations of U0126. Scale bar: 0.5 mm. (B) Q-PCR analysis of marker-gene expression. Their relative expression levels were compared to the levels in ES cells grown under normal serum-free culture conditions. (C) Morphology of hESCs cultured in activin A (100 ng/ml) plus FGF2 (10 ng/ml) treated with increasing concentrations of LY294002. Scale bar: 0.5 mm. (D) Q-PCR analysis of marker-gene expression. Their relative expression levels were compared to the levels in human ES cells grown in hESF9A.

Please cite this article as: Na, J., et al., Inhibition of ERK1/2 prevents neural and mesendodermal differentiation and promotes human embryonic stem cell self-renewal, Stem Cell Res. (2010), doi:10.1016/j.scr.2010.06.002

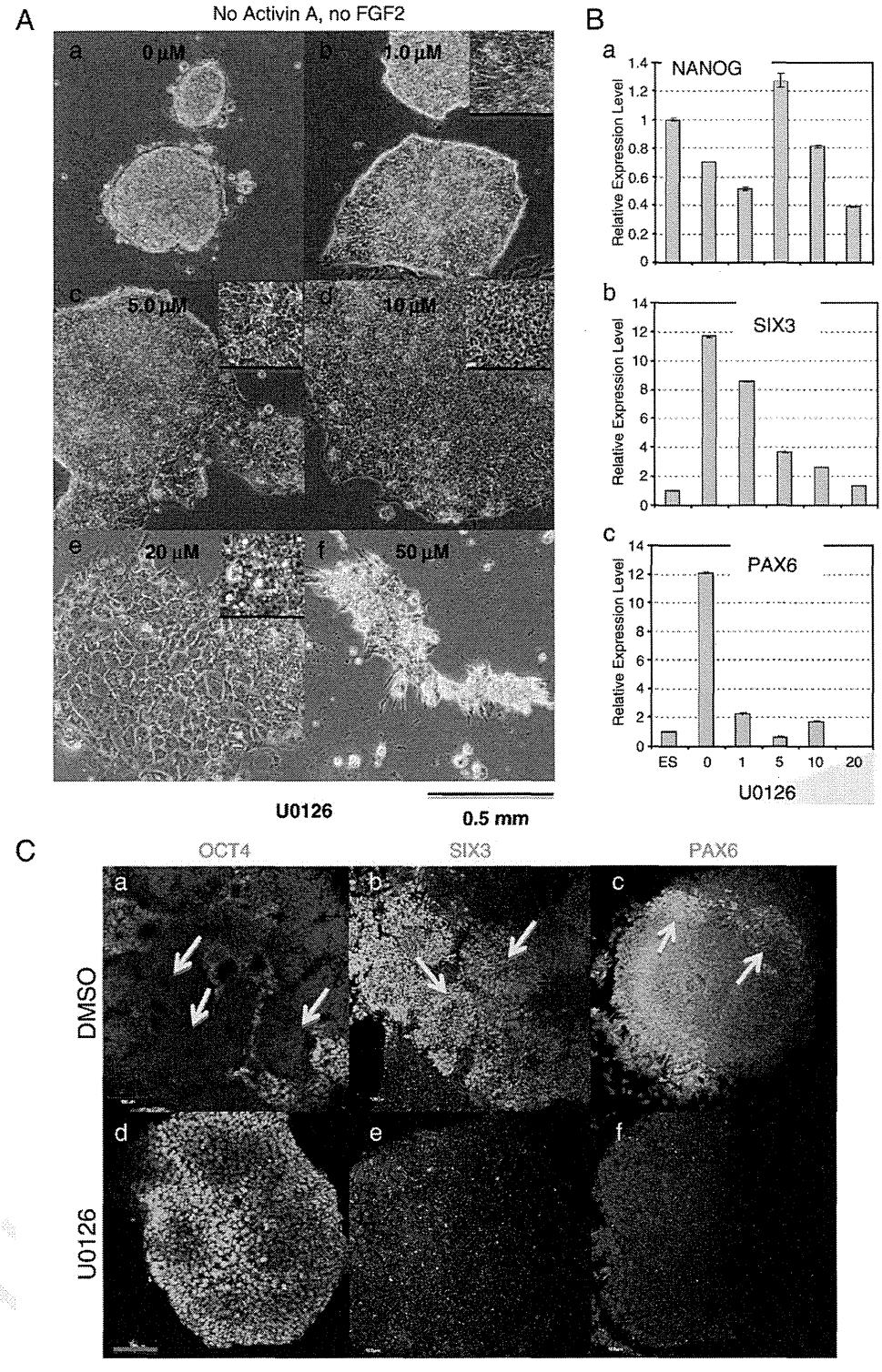

Figure 3 (A) Morphology of human ES cells cultured without activin A or FGF2 treated with increasing concentrations of U0126. Scale bar: 0.5 mm. Inset scale bar: 0.1 mm. (B) Q-PCR analysis of *NANOG*, *SIX3*, and *PAX6* expression. Their relative expression levels were compared to the levels in ES cells grown under normal serum-free culture conditions. (C) Immunostaining of OCT4, SIX3, and PAX6 (in green) in cells first treated without (a–c) or with U0126 (10 μM) (d–f) in hESF8 for 5 days, passaged, and then cultured in hESF9A. Note the absence of significant OCT4 staining in the absence of U0126, especially from the neural rosettes (panel a, arrows), and the retention of OCT4 expression the presence of U0126. By contrast, note the expression of SIX3 and PAX6, especially their nuclear localisation in the rosettes (arrows) in the absence of U0126 (panels b, c), but the absence of these transcription factors when the cells were cultured with U0126 (panels e, f). DNA: blue. Scale bar: 100 μm.

Please cite this article as: Na, J., et al., Inhibition of ERK1/2 prevents neural and mesendodermal differentiation and promotes human embryonic stem cell self-renewal, Stem Cell Res. (2010), doi:10.1016/j.scr.2010.06.002

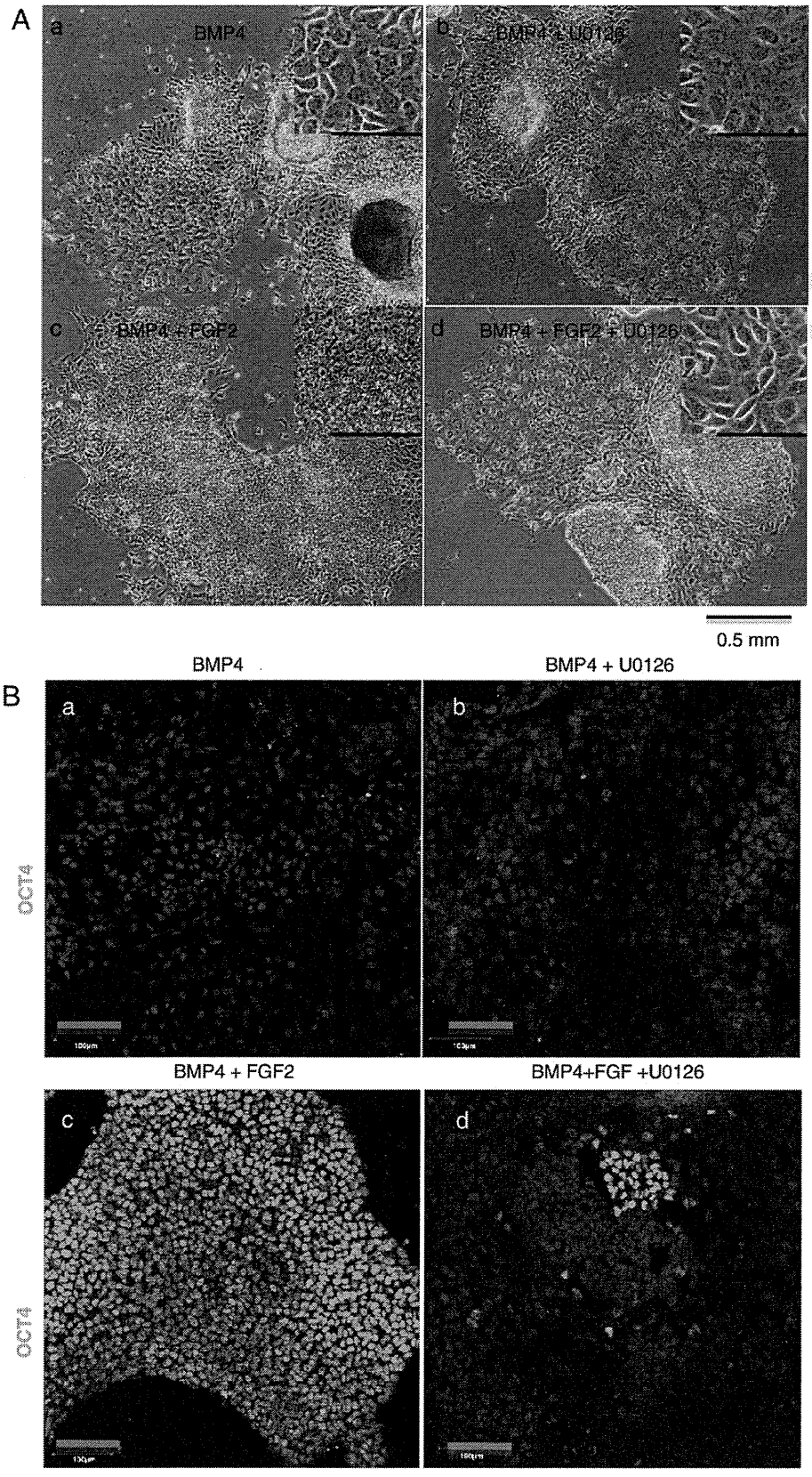

Figure 4 (A) Morphology of HUES1 cells cultured in different BMP4 (1 ng/ml), FGF2 (40 ng/ml), and U0126 (10 μM) combinations as indicated on the top of each graph. Scale bar: 0.5 mm. (B) Immunostaining of OCT4 (in green) of above experiment. DNA: blue. Scale bar: 100 μm.

Please cite this article as: Na, J., et al., Inhibition of ERK1/2 prevents neural and mesendodermal differentiation and promotes human embryonic stem cell self-renewal, Stem Cell Res. (2010), doi:10.1016/j.scr.2010.06.002

Long-term culture of human ES cells in a chemically defined medium containing U0126

Since U0126 can inhibit ES cell differentiation under chemically defined conditions, we assessed whether it can be used to support the self-renewal of several human ES cells during long-term culture in the hESF9A medium. To reduce the adverse effect of U0126 on cell adhesion, it was omitted from the medium when the cells were seeded as well as the following day; subsequently, cultures were fed with a medium containing U0126 until the next passage. After 3 passages (approx 3 weeks), three independent human ES cell lines, SHEF4, SHEF6, and the adapted HUES1 subline, grew to produce very large undifferentiated colonies in the hESF9A medium with 5 μM U0126 (Fig. 6A, panels a, c, and e), whereas without U0126 increased spontaneous differentiation was evident for the SHEF4 and SHEF6 cell lines (Fig. 6A, panels b and d). The adapted HUES1 subline also showed better colony morphology when cultured with U0126 (Fig. 6A, panel f). After culturing in U0126 for more than 3 months, SHEF4 and SHEF6 cells retained a normal karyotype, while no additional karyotype changes were detected in the adapted HUES1 line (Supplementary Fig. 6A). The SHEF4 and SHEF6 human ES cell lines expressed significantly higher levels of OCT4 and SSEA4 when grown in the presence of U0126 compared to nontreated cells (Fig. 6B). Adapted HUES1 cells displayed a less increased expression of OCT4 and SSEA4 when grown in the presence of U0126. This might reflect the innately different properties of individual human ES cell lines (Fig. 6B). To confirm the specificity of U0126, we used PD0325901, another ERK1/2 inhibitor used by

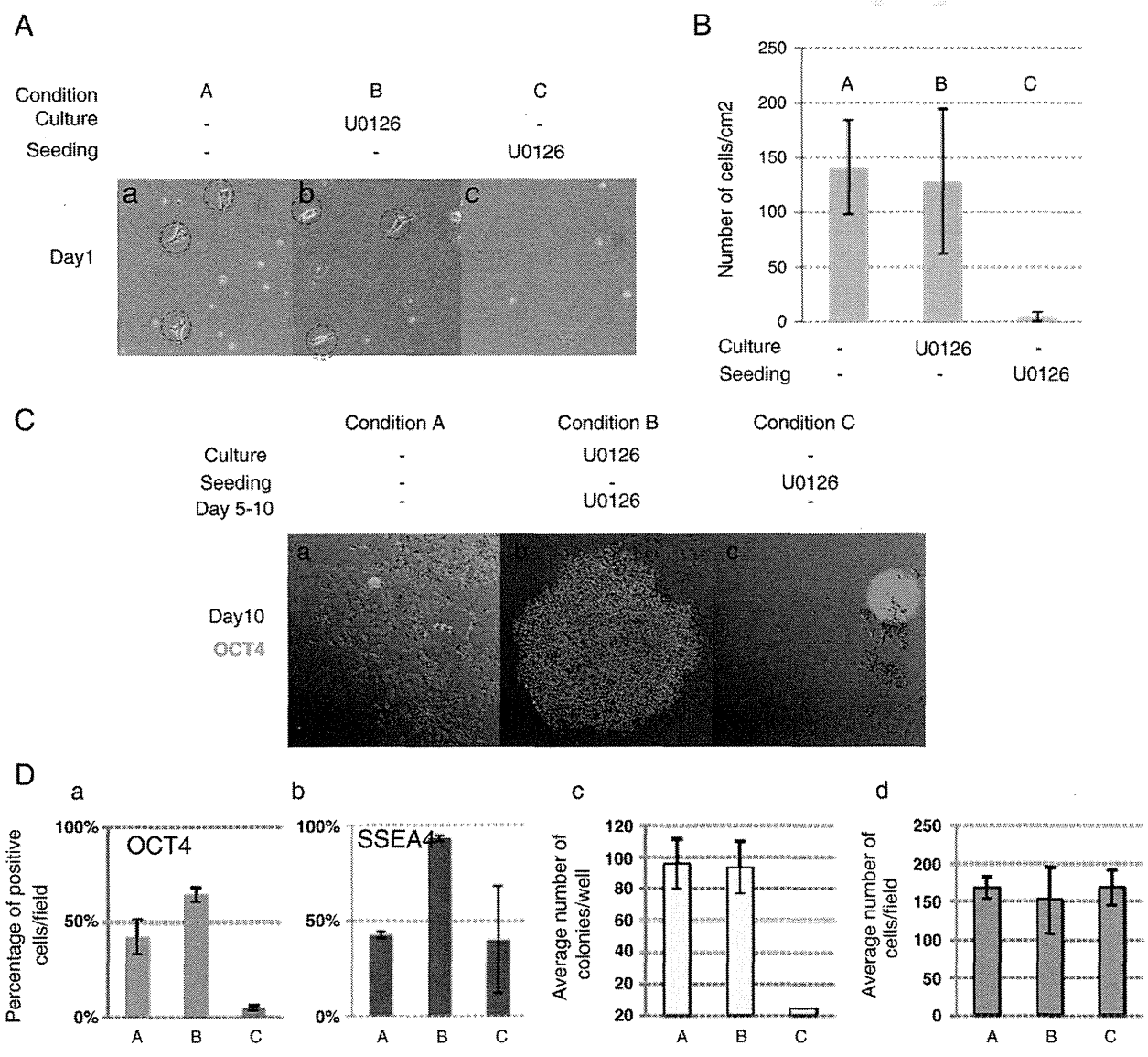

Figure 5 Inhibition of ERK1/2 prevented human ES cell attachment to the substrate. (A) Phase-contrast images of HUES1 cells attached to the substrate under different conditions (listed above each graph). (B) Bar-graph quantisation of HUES1 cell attachment after passaging with or without U0126. Seeding density was 2000 cells/cm^2. (C, a–c) Immunostaining of OCT4 expression under different conditions (listed above each graph). (D) Bar-graph presentation of the percentage of (a) OCT4- or (b) SSEA4-positive cells per field, (c) number of colonies per well, and (d) number of cells per field. The bars represent the mean of all measured colonies by the In Cell Analyser Developer's Toolbox and the error bar is the standard error of the mean (SEM).

Please cite this article as: Na, J., et al., Inhibition of ERK1/2 prevents neural and mesendodermal differentiation and promotes human embryonic stem cell self-renewal, Stem Cell Res. (2010), doi:10.1016/j.scr.2010.06.002

Ying and colleagues on mouse ES cells (Ying et al., 2008). We found that 0.3 μM PD0325901 was sufficient to block the phosphorylation of ERK1/2 in SHEF4 cells (Supplementary Fig. 6A). It reduced differentiation of the SHEF4 and SHEF6 cell lines during a period of 4 weeks (Supplementary Fig. 6B). Human ES cells cultured in PD0325901 or U0126 for 1–3 months retained the ability to undergo neural, mesendodermal, and extraembryonic differentiation when appropriate inducing conditions were applied. As shown in Supplementary Figs. 5B and 6D, differentiated cells strongly expressed TUJ1 (neural), BRACHYURY, FOXA2, SOX17 (mesendoderm), and CDX2 (extraembryonic) and downregulated OCT4. Our results show that the inhibition of ERK1/2 signaling helps to prevent differentiation of human ES cells in chemically defined environments and does not affect the pluripotency of these cells.

Discussion

In this study, we analysed the function of ERK1/2 in human ES cells under chemically defined culture conditions. Contrary to some previous reports that inhibition of ERK1/2 causes human ES cell differentiation (Li et al., 2007), our data demonstrate that inhibition of ERK1/2 signaling can be beneficial for self-renewal. Blocking ERK1/2 prevented mesendoderm and neural induction and, consequently, the

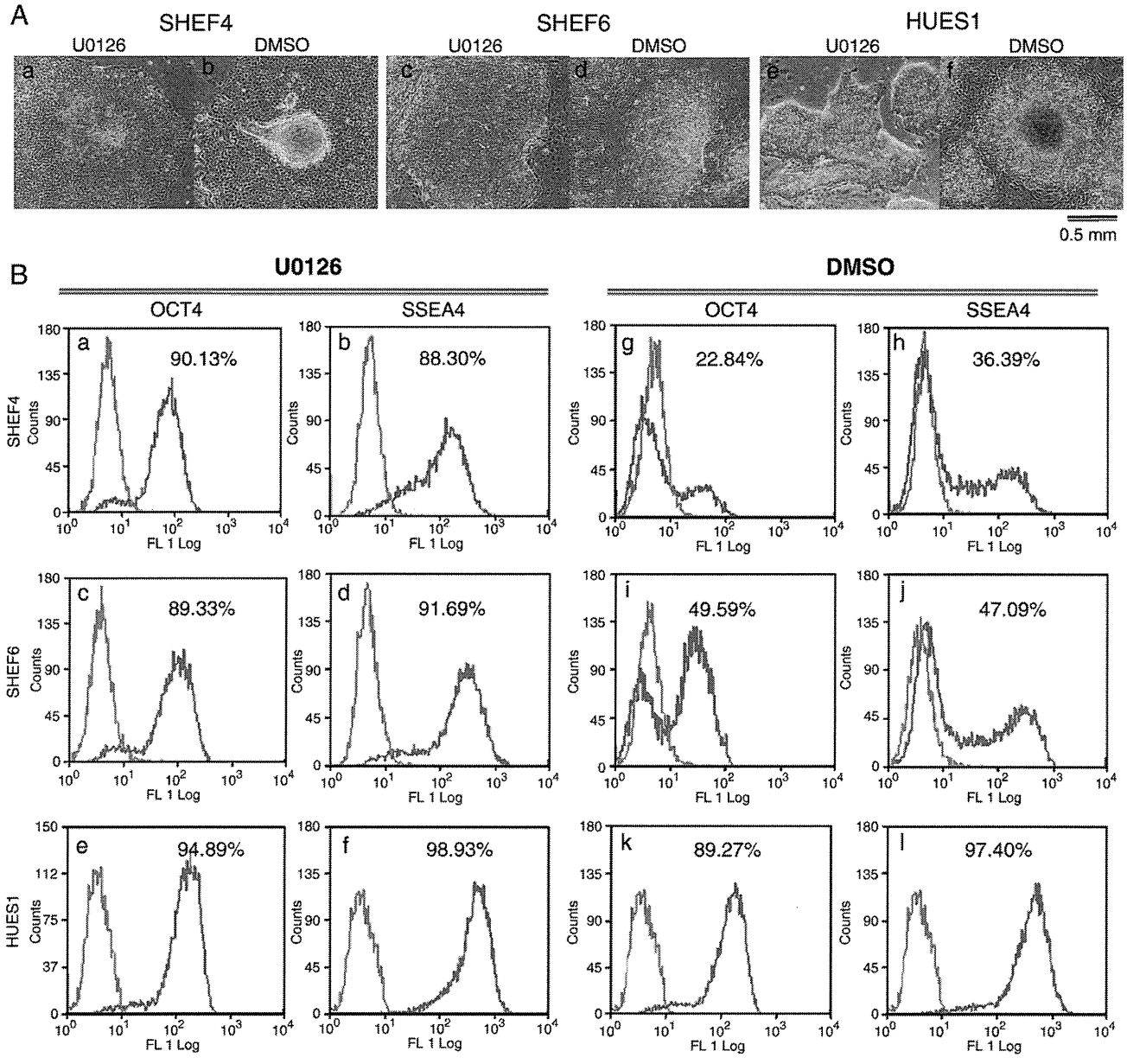

Figure 6 (A) Morphology of human ES cells cultured for 3 passages with or without U0126 in hESF9A. (B) FACS analysis of OCT4 and SSEA4 expression in human ES cells cultured with or without U0126 for 3 passages (3 weeks). The gray histogram is for SHEF4, SHEF6, and HUES1 cells stained with P3X (negative control). The red histograms represent the experimental population.

Please cite this article as: Na, J., et al., Inhibition of ERK1/2 prevents neural and mesendodermal differentiation and promotes human embryonic stem cell self-renewal, Stem Cell Res. (2010), doi:10.1016/j.scr.2010.06.002

ES cell phenotype was retained. However, ERK1/2 activation was needed to suppress BMP signaling under normal ES cell-culture conditions. Human ES cells retained OCT4 expression in the presence of a high dosage of FGF2 and 1 ng/ml of BMP4. When ERK1/2 inhibitor U0126 was added, cells rapidly differentiated toward an extraembryonic fate (Fig. 4). In this respect, human ES cells appear to be fundamentally different from mouse ES cells, as both FGF4 -/- and ERK2 -/- mouse ES cells were resistant to BMP4-induced differentiation (Kunath et al., 2007). This difference could explain why inhibition of ERK1/2 causes human ES cell differentiation in a KSR-containing medium that includes BMP-like activity (Xu et al., 2002, 2005). As the activation of ERK1/2 can suppress BMP signaling, blocking ERK in effect enhances BMP pathway activities and, consequently, cells differentiate toward extraembryonic fates. In a defined culture system supplemented with FGF2 and activin A but no exogenous BMP ligand, ERK1/2 is not required to suppress BMP signaling, and since inhibition of ERK1/2 stops both neural and mesendoderm differentiation, the cells will remain in the undifferentiated state.

In human ES cell cultures, FGF2 appeared to constitute some of the functions of LIF in mouse ES cells. In mice, parallel to the STAT3–JAK pathway that upregulates KLF4 and promotes pluripotency, LIF also activates both PI3K–AKT and MAPK1/2–ERK1/2 pathways (Niwa et al., 2009). AKT increases the expression level of the transcription factor TBX3, which is located upstream of the pluripotency factors NANOG and SOX2 (Niwa et al., 2009). On the other hand, the MAPK1/2–ERK1/2 pathway downregulates TBX3 and NANOG to encourage lineage commitment (Niwa et al., 2009). Both LIF and endogenously expressed FGF4 can elevate ERK activity, which gives ES cells a tendency to initiate spontaneous neural differentiation under serum- and feeder-free culture conditions (Stavridis et al., 2007; Ying et al., 2003a). In this scenario, addition of BMP4 suppressed neural differentiation by inducing the expression of Id proteins through SMAD1 (Ying et al., 2003b). Blocking ERK1/2 can prevent mouse ES cell neural differentiation and "trap" them in the "ground state" of self-renewal (Stavridis et al., 2007; Ying et al., 2008). In a separate study, Pluripotin, a small molecule that inhibits both ERK1/2 and Ras-GAP, was also able to sustain mouse ES cell self-renewal in the absence of BMP4 under chemically defined conditions, possibly through the same mechanism (Chen et al., 2006). Although LIF can stimulate STAT3 phosphorylation and, therefore, its activation, in human and primate ES cells this has no detectable effect on the pluripotency network (Daheron et al., 2004; Sumi et al., 2004). FGF2 strongly activates both AKT and ERK1/2. The AKT branch is critical for ES cell self-renewal. Watanabe and colleagues showed that overexpressing a constitutive active mutant form of AKT was able to maintain the self-renewal of both mouse and primate ES cells (Watanabe et al., 2006). In our experiments, inhibition of AKT through blocking PI3K accelerated mesendodermal differentiation of human ES cells under inducing conditions (Figs. 2C and D). Under chemically defined conditions, we found that ERK1/2 activation is required for proper neural and mesendodermal lineage specification. These two important functions seem to be conserved between human and mouse ES cells. ERK1/2 inhibition significantly reduces spontaneous differentiation as long as there is no BMP activity present and can thus serve as a useful strategy to maintain human ES cell self-renewal under defined conditions.

The interactions among ERK1/2, BMP, and TGFβ signaling pathways are complex and may depend on the relative levels of BMP and TGFβ signaling. It has been shown that ERK1/2 can phosphorylate the linker region of SMAD1 (a key transducer of BMP signals), and thus lead to its cytoplasmic retention and degradation (Fuentealba et al., 2007; Sapkota et al., 2007). Similarly, it can either directly phosphorylate SMAD2/3 or indirectly through other kinases such as CDK4/6, to regulate SMAD2/3 stability and subsequently the strength of TGFβ signaling (Schmierer and Hill, 2007). In a separate study from our laboratory by Avery et al., in a KSR-based medium inhibition of an activin A receptor-like kinase (ALK) strengthened BMP signaling, as indicated by stronger phosphorylation of the C-terminus of SMAD1/5/8 (its active form) and the upregulation of BMP-responsive genes such as MSX1. Knocking down SMAD4 reduced SMAD1/5/8 activation, abolished the upregulation of differentiation genes, and partially rescued the expression of the pluripotency genes OCT4 and NANOG (Avery et al., 2010). This implies that activin A/TGFβ signaling can sequester SMAD4 (the co-SMAD essential for both BMP and TGFβ pathways) from the BMP pathway, thus in effect attenuating the strength of the BMP activity. FGF2–ERK1/2 enhances activin A signaling and, in turn, antagonises BMP signaling and the associated extra-embryonic lineage differentiation. BMP4 is also reported to induce mesoderm differentiation from EBs (Takei et al., 2009). In this circumstance, the cell–cell interaction and the spatial organisation of the EBs may also have an impact on cell signaling and fate decisions.

MAPK–ERK1/2 signaling cascades also play critical roles in cell adhesion. In our experiments, U0126 markedly reduced cell attachment during passaging and prevented EMT during induced mesendodermal differentiation. Two recent publications showed that inhibition of FGF signaling affected human ES cell adhesion, which resulted in the upregulation of caspase 3 and anoikis, while a high concentration of FGF2 increased human ES cell clonogenicity and reduced the number of cells floating up in the culture (Eiselleova et al., 2009; Wang et al., 2009). ROCK inhibitor Y27632 could not rescue the reduction in cell adhesion caused by ERK1/2 inhibition (Supplementary Fig. 4). ERK1/2 inhibition is particularly detrimental to human ES cells when they are at low density. This is likely because cells are more dependent on the survival signal provided by cell–substrate adhesion. We noted that, as human ES cells grew to higher density, U0126 or PD0325901 treatment no longer impairs cell survival as much. Thus, close cell–cell contact must send out additional prosurvival signals. One of the candidate pathways is Notch signaling. RNAi knocking down of NOTCH1 and 2, or their canonical effector CBF-1, or blocking Notch signaling with the γ-secretase inhibitor L-685,458 all markedly reduced the growth of human ES cells (Fox et al., 2008). It has been shown that the engagement Notch receptor led to the activation of AKT, the transcription factor STAT3, and mammalian target of rapamycin to promote the survival of stem cells (Androutsellis-Theotokis et al., 2006). E-cadherin-mediated cell adhesion has also been shown to activate AKT though PI3K to stimulate epithelial cell growth (Pece et al., 1999). Therefore, cell–

Please cite this article as: Na, J., et al., Inhibition of ERK1/2 prevents neural and mesendodermal differentiation and promotes human embryonic stem cell self-renewal, Stem Cell Res. (2010), doi:10.1016/j.scr.2010.06.002

cell contact-dependent AKT activation may be able to compensate for the detrimental effect caused by ERK1/2 inhibition in human ES cells once they reach a certain density.

Based on our results, we propose that ERK1/2 plays multiple important roles in human ES cells (Fig. 7): it is required for neural and mesendoderm induction and essential for cell attachment to the substrate; however, it can suppress BMP signaling and prevent extraembryonic differentiation. Our model could explain the discrepancies regarding the roles of FGF2 and ERK1/2 in human ES cells and mouse ES cell self-renewal. Further dissecting the "balancing action" among FGF, BMP, and activin A/TGFβ pathways under chemically defined conditions will offer insights into how these developmental signals regulate mammalian ES cell fate decisions.

Materials and methods

Cell lines and maintenance

HUES1 (normal and adapted), SHEF4, SHEF5 and SHEF6 human ES cells were used in this study. SHEF4, SHEF5, and SHEF6 cells were maintained on feeders in an ES medium containing KO-DMEM (Invitrogen) supplemented with nonessential amino acids, 0.1 μM 2-mercaptoethanol, 1 mM glutamine, 20% serum replacement (Invitrogen), and 4 ng/ml FGF2 (Peprotech) (Amit et al., 2000). HUES1 cells were maintained on feeders in an HUES1 medium containing KO-DMEM supplemented with nonessential amino acids, 0.1 mM 2-mercaptoethanol, glutamine, 8% serum replacement, 8% plasminate (Bayer), and 4 ng/ml FGF2 (Cowan et al., 2004). In both cases, the cells were cultured at 37 °C in a humidified atmosphere of 5% CO_2 in air. The cells were passaged with 1 mg/ml collagenase IV (Invitrogen) (for SHEF lines) and 0.05% trpsin/0.04% EDTA (Sigma) (for HUES1), respectively. The cells were seeded onto a 25 cm^2 flask (NUNC) that had been previously coated with 0.1% porcine gelatin (Sigma) and mitomycin C (Sigma)-inactivated MEF as feeder cells.

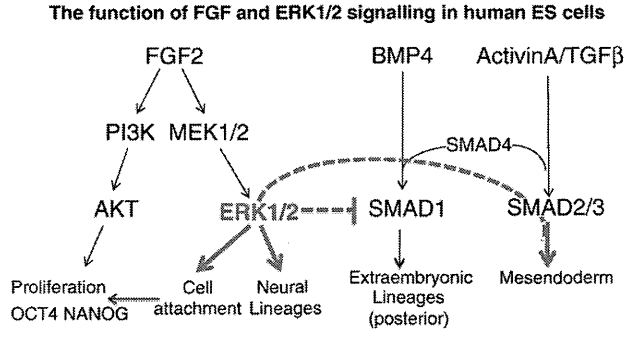

Figure 7 Model depicting multiple roles of ERK1/2 in human ES cells. FGF2 activated both AKT and ERK1/2. ERK1/2 promotes neural and mesendodermal (together with a high dosage of activin A/TGFβ) differentiation from ES cells while it suppresses BMP-induced extraembryonic lineage differentiation. It is also needed for human ES cell attachment to the substrate, which is essential for ES cell survival and proliferation.

Human ES cell culture in serum-free, feeder-free, and chemically defined medium

Prior to growth-factor-treatment experiments, human ES cells were grown for more than 3 passages in the absence of feeders in a serum-free and chemically defined medium on type I collagen gel (Nita Gelatin, Japan) (Furue et al., 2008). The hESF basal medium was purchased from the Cell Science & Technology Institute Inc., Sendai, Japan. The components of hESF8, 9, and 9A are listed in Supplementary Table 1. Because cells are very sensitive to the passaging strategy used, including the size of colonies that are passaged, the addition of activin A permits the maintenance of more robust and reproducible cultures of undifferentiated cells. Thus, hESF9A containing 10 ng/ml of FGF2 and activin A each was used for regular serum-free culture. Before the start of each series of experiments, when necessary, manual passaging was used to ensure a uniform undifferentiated starting cell population for all treatment groups.

Growth-factor treatment and differentiation protocols

Serum-free, feeder-free cultured human ES cells were seeded in 12-well plates at a density of 4×10^4/well. One day after seeding, the cells were washed with an hESF8 medium, and then fed with hESF8 and with activin A (R&D systems), BMP4, and FGF2 (Peprotech) added at the desired concentrations. The medium was changed every 2 days with freshly added growth factors. Cells were collected after 5 days and analysed. For neural differentiation, we used a protocol modified from Zhang et al. (2001). Briefly, SHEF4 and SHEF6 cells were first cultured as floating EBs in hESF8 with 4 ng/ml of FGF2 for 1 week. These EBs were then plated in 6-well plates coated with poly-L-ornithine hydrobromide (PLOH) and 2 μg/cm^2 Laminin (LN) (Sigma) and fed with hESF8 and 20 ng/ml of FGF for 1 week. Afterward, colonies with neural rosette morphology were manually picked and cultured in suspension in the same medium for another 7 days. These rosettes were replated on a PLOH/LN surface for 7–10 days. Rosettes with extensively long neurites were picked and dissociated to obtain a relatively pure population of neuronal cells. To initiate mesendodermal or extraembryonic differentiation, cells were treated with 100 ng/ml activin A plus 10 ng/ml FGF2 or 10 ng/ml of BMP4 on 2 μg/cm^2 FN-coated surface for 7 days.

Antibodies and chemical inhibitors

The following antibodies were used in this study: SMAD4, OCT4, ERK1/2, and BRACHYURY (Santa Cruz); CDX2, FOXA2, NANOG, and SOX17 (R&D systems); SIX3 (a rabbit polyclonal antibody raised against polypeptide RLQ HQA IGP SGM RSL AEP GC which corresponds to the C terminus of mouse SIX3; the same sequence was present in human SIX3); PAX6 and FORSE1 (Developmental Studies Hybridoma Bank, IA, USA); phospho-ERK1/2, phospho-AKT, phospho-GSK3β, total GSK3 β (Cell Signaling); SOX2 and actin (Abcam, Cambridge UK). The monoclonal antibody to SSEA4 was produced from a culture of hybridoma 813-70 (Kannagi et al., 1983). The chemical inhibitors U0126, LY294002, and PD0325901 were

Please cite this article as: Na, J., et al., Inhibition of ERK1/2 prevents neural and mesendodermal differentiation and promotes human embryonic stem cell self-renewal, Stem Cell Res. (2010), doi:10.1016/j.scr.2010.06.002

purchased from Promega, Merck, and AXON Medchem (Groningen, the Netherlands), respectively.

Western blot

For Western blot analysis, HUES1 cells were first cultured in hESF9A for 48 h and then washed briefly with PBS and cultured in hESF8 (without FGF and activin A) for 48 h. Afterward, 10 ng/ml of FGF2 and chemical inhibitors (U0126 10 μM, LY294002 10 μM, PD0325901 0.3 μM, or DMSO only) were added, while 30 min later cells were detached and lysed on ice in a sample-loading buffer (0.125 M Tris-HCl, pH 6.8, 4% SDS, 20% glycerol, PhosSTOP (Roche), and 0.002% bromophenol blue). The amount of 2×10^5 cells-equivalent lysate was loaded per lane.

Quantitative PCR

Total RNA was extracted with TRIZOL (Invitrogen). The amount of 1 μg RNA of each sample was used for reverse transcription (20 μl) using Superscript III (Invitrogen). Q-PCRs were performed using SYBR Green JumpStart Taq ReadyMix (Sigma-Aldrich) in an iCycler (Bio-Rad). Each gene was done in triplicate (Fig. 1) or duplicate (Figs. 2 and 3). The sample input was normalised against the C_t (critical threshold) value of the housekeeping gene GAPDH. Relative quantification of each gene was performed using the iCycler Excel program. The error bar is the standard deviation of the C_t value. Primer sequences are listed in Supplementary Table 2.

Immunostaining, FACS, and high-content screen

For in situ immunostaining and high-content screen, cells were fixed in 6-well plates with 4% PFA in PBS. OCT4 and SSEA4 staining was scanned in an In Cell Analyser 1000 (Amersham Biosciences) and analysed using the Developer's Toolbox. OCT4, SIX3, and PAX6 staining was imaged with an Olympus FV1000 confocal microscope. For FACS analysis, cells were incubated with 0.05% trypsin in 0.2% EDTA in 37 °C, 10% CO_2 incubator until most dissociated into single cells. Trypsin inhibitor (Sigma T6522) (1 mg/ml in DMEM) was immediately added to inactivate the trypsin. Cells were subsequently rinsed off the flask or 6-well plate with an hESF8 medium, centrifuged down, and washed 3 times in PBS containing 4 mg/ml polyvinylpyrrolidone (Sigma) to prevent them from sticking together. They were fixed in 4% PFA in PBS 0.1% Tween 20 (PBST) for 20 min at room temperature. For intracellular staining of Oct4, 0.2% Triton X-100 was included in the fixative. Afterward, cells were washed 3 times in PBST, blocked with 5% FBS–PBST for 1 h, and incubated with the desired primary and secondary antibodies. FACS was done using a DAKO Cytomation $CyAn_{ADP}$ machine.

Y27632 treatment and clonogenicity assay

SHEF6 cells were dissociated into single cells as described above and seeded at 10,000 cells/cm^2 in FN (2 μg/cm^2) coated 6-well plates in hESF9A. Y27632 (10 μM) or U0126 (10 μM) was added 2 h prior to passaging and overnight during seeding as described in Watanabe et al. (2007). The medium was replaced the next day. Cells were grown in hESF9A for another 10 days, then fixed briefly, and stained with alkaline phosphatase (AP) Red Substrate Solution (Sigma). AP-positive colonies were photographed and counted.

Uncited reference

Harb et al., 2008 Q1

Acknowledgments

This work was supported by a Medical Research Council Collaborative Career Development Fellowship in Stem Cell Research to J.N., and grants from the MRC and ESTOOLS, an integrated project of the 6th Framework Programme of the European Commission. We thank Dr. M. Jones, Mr. D. Harley, and Dr. P. Gokhale for assistance with FACS and high-content screen analysis, Prof. Harry Moore for providing SHEF cell lines, and Prof. Marysia Placzek for SIX3 antibody. Confocal images were acquired using the Light Microscopy Facility funded by the Wellcome Trust (Grant GR077544AIA).

Appendix A. Supplementary data

Supplementary data associated with this article can be found, in the online version, at 10.1016/j.scr.2010.06.002.

References

Amit, M., Carpenter, M.K., Inokuma, M.S., Chiu, C.P., Harris, C.P., Waknitz, M.A., Itskovitz-Eldor, J., Thomson, J.A., 2000. Clonally derived human embryonic stem cell lines maintain pluripotency and proliferative potential for prolonged periods of culture. Dev. Biol. 227, 271–278.

Androutsellis-Theotokis, A., Leker, R.R., Soldner, F., Hoeppner, D. J., Ravin, R., Poser, S.W., Rueger, M.A., Bae, S.K., Kittappa, R., McKay, R.D., 2006. Notch signalling regulates stem cell numbers in vitro and in vivo. Nature 442, 823–826.

Avery, S., Zafarana, G., Gokhale, P.J., Andrews, P.W., 2010. The Role of SMAD4 in human embryonic stem cell self-renewal and stem cell fate. Stem Cells.

Bain, J., Plater, L., Elliott, M., Shpiro, N., Hastie, C.J., McLauchlan, H., Klevernic, I., Arthur, J.S., Alessi, D.R., Cohen, P., 2007. The selectivity of protein kinase inhibitors: a further update. Biochem. J. 408, 297–315.

Burdon, T., Stracey, C., Chambers, I., Nichols, J., Smith, A., 1999. Suppression of SHP-2 and ERK signalling promotes self-renewal of mouse embryonic stem cells. Dev. Biol. 210, 30–43.

Chazaud, C., Yamanaka, Y., Pawson, T., Rossant, J., 2006. Early lineage segregation between epiblast and primitive endoderm in mouse blastocysts through the Grb2-MAPK pathway. Dev. Cell 10, 615–624.

Chen, S., Do, J.T., Zhang, Q., Yao, S., Yan, F., Peters, E.C., Scholer, H. R., Schultz, P.G., Ding, S., 2006. Self-renewal of embryonic stem cells by a small molecule. Proc. Natl. Acad. Sci. USA 103, 17266–17271.

Ciruna, B., Rossant, J., 2001. FGF signaling regulates mesoderm cell fate specification and morphogenetic movement at the primitive streak. Dev. Cell 1, 37–49.

Corson, L.B., Yamanaka, Y., Lai, K.M., Rossant, J., 2003. Spatial and temporal patterns of ERK signaling during mouse embryogenesis. Development 130, 4527–4537.

Please cite this article as: Na, J., et al., Inhibition of ERK1/2 prevents neural and mesendodermal differentiation and promotes human embryonic stem cell self-renewal, Stem Cell Res. (2010), doi:10.1016/j.scr.2010.06.002

Cowan, C.A., Klimanskaya, I., McMahon, J., Atienza, J., Witmyer, J., Zucker, J.P., Wang, S., Morton, C.C., McMahon, A.P., Powers, D., Melton, D.A., 2004. Derivation of embryonic stem-cell lines from human blastocysts. N Engl J. Med. 350, 1353–1356.

Daheron, L., Opitz, S.L., Zaehres, H., Lensch, M.W., Andrews, P.W., Itskovitz-Eldor, J., Daley, G.Q., 2004. LIF/STAT3 signaling fails to maintain self-renewal of human embryonic stem cells. Stem Cells 22, 770–778.

D'Amour, K.A., Agulnick, A.D., Eliazer, S., Kelly, O.G., Kroon, E., Baetge, E.E., 2005. Efficient differentiation of human embryonic stem cells to definitive endoderm. Nat. Biotechnol. 23, 1534–1541.

Dreesen, O., Brivanlou, A.H., 2007. Signaling pathways in cancer and embryonic stem cells. Stem Cell Rev. 3, 7–17.

Eiselleova, L., Matulka, K., Kriz, V., Kunova, M., Schmidtova, Z., Neradil, J., Tichy, B., Dvorakova, D., Pospisilova, S., Hampl, A., Dvorak, P., 2009. A complex role for FGF-2 in self-renewal, survival, and adhesion of human embryonic stem cells. Stem Cells 27, 1847–1857.

Fox, V., Gokhale, P.J., Walsh, J.R., Matin, M., Jones, M., Andrews, P.W., 2008. Cell-cell signaling through NOTCH regulates human embryonic stem cell proliferation. Stem Cells 26, 715–723.

Fuentealba, L.C., Eivers, E., Ikeda, A., Hurtado, C., Kuroda, H., Pera, E.M., De Robertis, E.M., 2007. Integrating patterning signals: Wnt/GSK3 regulates the duration of the BMP/Smad1 signal. Cell 131, 980–993.

Furue, M.K., Na, J., Jackson, J.P., Okamoto, T., Jones, M., Baker, D., Hata, R., Moore, H.D., Sato, J.D., Andrews, P.W., 2008. Heparin promotes the growth of human embryonic stem cells in a defined serum-free medium. Proc. Natl. Acad. Sci. USA 105, 13409–13414.

Harb, N., Archer, T.K., Sato, N., 2008. The Rho-Rock-Myosin signaling axis determines cell-cell integrity of self-renewing pluripotent stem cells. PLoS ONE 3, e3001.

Johnson, G.L., Lapadat, R., 2002. Mitogen-activated protein kinase pathways mediated by ERK, JNK, and p38 protein kinases. Science 298, 1911–1912.

Kannagi, R., Cochran, N.A., Ishigami, F., Hakomori, S., Andrews, P. W., Knowles, B.B., Solter, D., 1983. Stage-specific embryonic antigens (SSEA-3 and -4) are epitopes of a unique globo-series ganglioside isolated from human teratocarcinoma cells. EMBO J. 2, 2355–2361.

Kunath, T., Saba-El-Leil, M.K., Almousailleakh, M., Wray, J., Meloche, S., Smith, A., 2007. FGF stimulation of the Erk1/2 signalling cascade triggers transition of pluripotent embryonic stem cells from self-renewal to lineage commitment. Development 134, 2895–2902.

Li, J., Wang, G., Wang, C., Zhao, Y., Zhang, H., Tan, Z., Song, Z., Ding, M., Deng, H., 2007. MEK/ERK signaling contributes to the maintenance of human embryonic stem cell self-renewal. Differentiation 75, 299–307.

Li, P., Tong, C., Mehrian-Shai, R., Jia, L., Wu, N., Yan, Y., Maxson, R. E., Schulze, E.N., Song, H., Hsieh, C.L., Pera, M.F., Ying, Q.L., 2008. Germline competent embryonic stem cells derived from rat blastocysts. Cell 135, 1299–1310.

Morrison, G.M., Oikonomopoulou, I., Migueles, R.P., Soneji, S., Livigni, A., Enver, T., Brickman, J.M., 2008. Anterior definitive endoderm from ESCs reveals a role for FGF signaling. Cell Stem Cell 3, 402–415.

Nichols, J., Jones, K., Phillips, J.M., Newland, S.A., Roode, M., Mansfield, W., Smith, A., Cooke, A., 2009. Validated germline-competent embryonic stem cell lines from nonobese diabetic mice. Nat. Med.

Niwa, H., Ogawa, K., Shimosato, D., Adachi, K., 2009. A parallel circuit of LIF signalling pathways maintains pluripotency of mouse ES cells. Nature 460, 118–122.

Pece, S., Chiariello, M., Murga, C., Gutkind, J.S., 1999. Activation of the protein kinase Akt/PKB by the formation of E-cadherin-mediated cell-cell junctions. Evidence for the association of phosphatidylinositol 3-kinase with the E-cadherin adhesion complex. J. Biol. Chem. 274, 19347–19351.

Pera, M.F., Andrade, J., Houssami, S., Reubinoff, B., Trounson, A., Stanley, E.G., Ward-van Oostwaard, D., Mummery, C., 2004. Regulation of human embryonic stem cell differentiation by BMP-2 and its antagonist noggin. J. Cell Sci. 117, 1269–1280.

Sapkota, G., Alarcon, C., Spagnoli, F.M., Brivanlou, A.H., Massague, J., 2007. Balancing BMP signaling through integrated inputs into the Smad1 linker. Mol. Cell 25, 441–454.

Schmierer, B., Hill, C.S., 2007. TGFbeta-SMAD signal transduction: molecular specificity and functional flexibility. Nat. Rev. Mol. Cell Biol. 8, 970–982.

Sperger, J.M., Chen, X., Draper, J.S., Antosiewicz, J.E., Chon, C.H., Jones, S.B., Brooks, J.D., Andrews, P.W., Brown, P.O., Thomson, J.A., 2003. Gene expression patterns in human embryonic stem cells and human pluripotent germ cell tumors. Proc. Natl. Acad. Sci. USA 100, 13350–13355.

Stavridis, M.P., Lunn, J.S., Collins, B.J., Storey, K.G., 2007. A discrete period of FGF-induced Erk1/2 signalling is required for vertebrate neural specification. Development 134, 2889–2894.

Sumi, T., Fujimoto, Y., Nakatsuji, N., Suemori, H., 2004. STAT3 is dispensable for maintenance of self-renewal in nonhuman primate embryonic stem cells. Stem Cells 22, 861–872.

Takei, S., Ichikawa, H., Johkura, K., Mogi, A., No, H., Yoshie, S., Tomotsune, D., Sasaki, K., 2009. Bone morphogenetic protein-4 promotes induction of cardiomyocytes from human embryonic stem cells in serum-based embryoid body development. Am. J. Physiol. Heart Circ. Physiol. 296, H1793–H1803.

Tanaka, S., Kunath, T., Hadjantonakis, A.K., Nagy, A., Rossant, J., 1998. Promotion of trophoblast stem cell proliferation by FGF4. Science 282, 2072–2075.

Wang, X., Lin, G., Martins-Taylor, K., Zeng, H., Xu, R.H., 2009. Inhibition of caspase-mediated anoikis is critical for basic fibroblast growth factor-sustained culture of human pluripotent stem cells. J. Biol. Chem. 284, 34054–34064.

Watanabe, S., Umehara, H., Murayama, K., Okabe, M., Kimura, T., Nakano, T., 2006. Activation of Akt signaling is sufficient to maintain pluripotency in mouse and primate embryonic stem cells. Oncogene 25, 2697–2707.

Watanabe, K., Ueno, M., Kamiya, D., Nishiyama, A., Matsumura, M., Wataya, T., Takahashi, J.B., Nishikawa, S., Muguruma, K., Sasai, Y., 2007. A ROCK inhibitor permits survival of dissociated human embryonic stem cells. Nat. Biotechnol. 25, 681–686.

Xu, R.H., Chen, X., Li, D.S., Li, R., Addicks, G.C., Glennon, C., Zwaka, T.P., Thomson, J.A., 2002. BMP4 initiates human embryonic stem cell differentiation to trophoblast. Nat. Biotechnol. 20, 1261–1264.

Xu, R.H., Peck, R.M., Li, D.S., Feng, X., Ludwig, T., Thomson, J.A., 2005. Basic FGF and suppression of BMP signaling sustain undifferentiated proliferation of human ES cells. Nat. Methods 2, 185–190.

Yao, Y., Li, W., Wu, J., Germann, U.A., Su, M.S., Kuida, K., Boucher, D.M., 2003. Extracellular signal-regulated kinase 2 is necessary for mesoderm differentiation. Proc. Natl. Acad. Sci. USA 100, 12759–12764.

Ying, Q.L., Stavridis, M., Griffiths, D., Li, M., Smith, A., 2003a. Conversion of embryonic stem cells into neuroectodermal precursors in adherent monoculture. Nat. Biotechnol. 21, 183–186.

Ying, Q.L., Nichols, J., Chambers, I., Smith, A., 2003b. BMP induction of Id proteins suppresses differentiation and sustains embryonic stem cell self-renewal in collaboration with STAT3. Cell 115, 281–292.

Ying, Q.L., Wray, J., Nichols, J., Batlle-Morera, L., Doble, B., Woodgett, J., Cohen, P., Smith, A., 2008. The ground state of embryonic stem cell self-renewal. Nature 453, 519–523.

Zhang, S.C., Wernig, M., Duncan, I.D., Brustle, O., Thomson, J.A., 2001. In vitro differentiation of transplantable neural precursors from human embryonic stem cells. Nat. Biotechnol. 19, 1129–1133.

Please cite this article as: Na, J., et al., Inhibition of ERK1/2 prevents neural and mesendodermal differentiation and promotes human embryonic stem cell self-renewal, Stem Cell Res. (2010), doi:10.1016/j.scr.2010.06.002

In Vitro Cell.Dev.Biol.—Animal (2010) 46:573–576
DOI 10.1007/s11626-010-9317-z

LETTER

Advantages and difficulties in culturing human pluripotent stem cells in growth factor-defined serum-free medium

Miho Kusuda Furue · Daiki Tateyama · Masaki Kinehara · Jie Na · Tetsuji Okamoto · J. Denry Sato

Received: 25 March 2010 / Accepted: 5 April 2010 / Published online: 29 April 2010 / Editor: J. Denry Sato

Dear Editor,

Serum- and feeder-free culture conditions have received a great deal of attention for culturing human embryonic stem (hES) cells or induced pluripotent stem (iPS) cells although hES/iPS cells are still most commonly maintained on inactivated mouse embryonic fibroblast feeders (MEF) in medium supplemented with FBS (Thomson et al. 1998; Reubinoff et al. 2000), or proprietary replacements, such as knockout serum replacement (KSR) together with fibroblast growth factor-2 (FGF-2) (Amit et al. 2000; Draper et al. 2004). Use of culture media containing undefined or undisclosed components has limited the development of applications for pluripotent cells because of our lack of knowledge of their responses to specific cues that control self-renewal, differentiation, and lineage selection. Therefore, a defined serum-free medium consisting of minimum essential components for culturing hES/iPS cells could contribute to advances in the field.

Previously, we have developed a defined growth factor-supplemented serum-free medium, hESF9, for the culture of human ES cells on a type I collagen substrate without feeders (Furue et al. 2008). This medium consists of hESF basal medium supplemented with heparin and only four protein components: insulin, transferrin, albumin conjugated with oleic acid, and FGF-2 (10 ng/ml). Under these culture conditions, FGF-2 promotes proliferation of hES cells in a concentration-dependent manner. Heparin, which is known to enhance the activity of FGF, also promotes proliferation of hES cells in a concentration-dependent manner in the absence of FGF-2 suggesting that endogenous FGF-2 is produced by hES cells. In conventional cultures with KSR-based medium, the proliferative effects of FGF-2 or heparin are not detectable although it is well known that FGF-2 supports hES cell growth. Thus, a defined serum-free medium consisting of minimum essential components could aid in elucidating hES/iPS cell responses to specific cues that control self-renewal, differentiation, and lineage selection.

The modern era of serum-free growth began in the mid-1970s when Izumi Hayashi and Gordon Sato (1976) defined conditions for growth of a rat pituitary cell line in a hormonally defined serum-free medium that did not alter cell phenotypes or cell growth. N2 supplements for neural

M. Kusuda Furue · D. Tateyama · M. Kinehara
Laboratory of Cell Cultures, Division of Bioresources,
National Institute of Biomedical Innovations,
Osaka 567-0085, Japan

M. Kusuda Furue (✉)
Laboratory of Cell Processing,
Institute for Frontier Medical Sciences, Kyoto University,
Kyoto 606-8507, Japan
e-mail: mkfurue@nibio.go.jp

J. Na
School of Medicine, Tsinghua University,
Beijing, China

T. Okamoto
Department of Molecular Oral Medicine and Maxillofacial Surgery, Division of Frontier Medical Sciences,
Graduate Science School of Biomedical Sciences,
Hiroshima University,
Hiroshima 734-8553, Japan

J. D. Sato
Mount Desert Island Biological Laboratory,
Salisbury Cove, ME 04672, USA

J. Na
The Centre for Stem Cell Biology,
The University of Sheffield,
Sheffield, S10 2TN,
United Kingdom

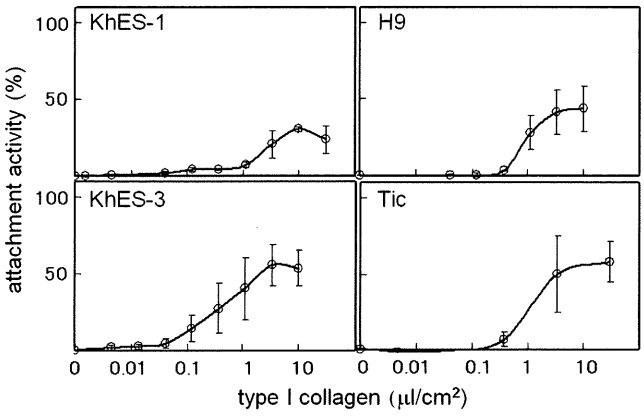

Figure 1. Attachment and proliferation of hES and iPS cells on type I collagen. The attachment of hES/iPS cells to ECM components was measured by the procedures followed by Fassler and Meyer (1995). Briefly, a 96-well microplate (Corning Costar, Corning, NY) was coated with each adhesion molecule at 37°C for 3 h. hES/iPS cells were seeded at confluent density (3×10^6cells cm^{-2}) on type I collagen (Nitta Gelatin, Inc.) coated plates in hESF9 (Cell Science & Technology Institute, Inc.). After 3 d, the attached cells were fixed and stained for 30 min with 0.4% crystal violet (Sigma) in methanol. After the plate was washed and dried, a solution (1% acetic acid and 30% ethanol in water) was added to the wells to dissolve the crystal violet. The absorbance of 595 nm, which indicated the concentration of the dissolved crystal violet, was measured with a microplate reader (model 550; Bio-Rad, Hercules, CA). Each graph shows the percentage of the attached cells on type I collagen in hESF9 relative to the attached cells on fibronectin (Sigma) as 100% as all the cell lines attached to fibronectin in hESF9. *Bar*=SE (n=3).

cells were developed by Bottenstein and Sato (1979). Later, we described a variety of serum-free media that can be used to propagate and analyze differentiated cells (Barnes and Sato 1980; Sato 1987; Furue et al. 1994; Okamoto et al. 1996; Sato et al. 2002). Serum contains variable amounts of hormones, soluble growth and differentiation factors, attachment factors, and undefined components. Also MEFs secrete a variety of nutrients or growth factors most of which have not been identified. The precise formulation of KSR is not in the public domain, and although "serum-free," it is likely to contain a variety of animal products (PCT/US98/00467; WO98/30679). The formulations of several other products for serum-free culture from several companies are also proprietary. These undefined or disclosed components of the culture conditions hamper analysis of the mechanisms that control cell behavior.

However, there are several difficulties in culturing hES/iPS cells in defined conditions without MEFs. First, propagation of pluripotent hES/iPS cells has been difficult to achieve even in conventional culture media due to their propensity to differentiate (Skottman and Hovatta 2006; Adewumi et al. 2007) as most researchers working with hES/iPS cells know. When cells grown to confluence are split, many differentiated cells appear in the next passage. The variability of batches of MEFs or KSR affects the tendency of cells to differentiate. The dissociation method is the most problematic. Even in conventional cell culture, imprecise handling during dissociation decreases cell survival as single hES/iPS cells cannot survive. Centrifugation at high speed decreases cell survival or promotes cell aggregation. Unless the cells are handled with care for several passages on MEFs in KSR-based medium, the cells do not survive or differentiate when transferred to feeder-free cultures. We had used EDTA to dissociate hES cell colonies in the feeder-free culture method using hESF9 medium. As the attachment activity of undifferentiated hES cells is different from that of differentiated cells, the undifferentiated hES cells were able to be transferred to the next passage, which led to the successful continuous culture of undifferentiated cells. However, this method requires previous practical experience with human primary

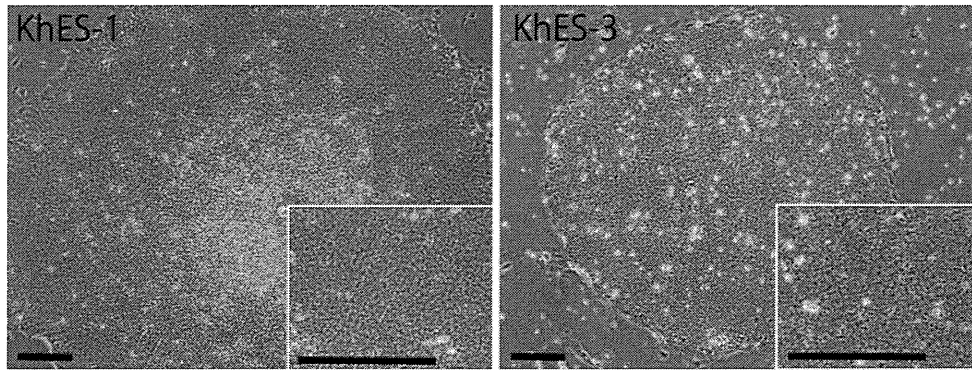

Figure 2. hES cells cultured on fibronectin in hESF9 medium. Phase-contrast microphotographs of KhES-1 at passage 16 and KhES-3 at passage 6 cultured on fibronectin in hESF9 medium. After 2 d, the KhES-1 cells and KhES-3 cells (from Kyoto University) cultured on MEF in KSR-based medium were passaged by the routine procedure onto the new MEF; the medium was changed to hESF9 medium, and then the cells were cultured on MEF for more than 4 d. Previously, we dissociated the hES cells with EDTA, but some of cell lines could not survive after the dissociation with EDTA. Then, we have utilized 1 U/ml dispase (Roche Applied Science) for approximately 1 min at 37°C to dissociate the hES/iPS colonies into the small clumps. The cells were washed twice at 20 g and then seeded on fibronectin-coated flask (Corning Costar) in hESF9 medium.

cell cultures. As hESF9 medium consists of minimum essential components, improper handling greatly affects cell viability and culture outcome.

Second, there are variations in the characteristics of hES/iPS cell lines as most of the researchers working on hES/iPS cells have come to realize. hES cell lines, Shef1, Shef5, and HUES1 cultured in the University of Sheffield were able to attach to type I collagen and grow well in hESF9 medium (Furue et al. 2008). However, we found that attachment activity of the KhES-1 line (Nakatsuji 2005), which was established in Kyoto University, to type I collagen seemed low, suggesting that there is a difference between the cell lines in their attachment ability. Owing to regulatory issues for hES cell importation into Japan, we were unable to directly compare KhES-1 cells with Shef1 or HUES1. We have examined the attachment and growth activity of other hES lines (KhES-3 from Kyoto University, Kyoto, Japan; H9 from National Stem Cell Bank, WiCell, Madison, WI) and the MRC-5-derived iPS cell line Tic (JCRB 1331, JCRB Cell Bank, Osaka, Japan), which was established in the National Center for Child Health and Development, on type I collagen (Nitta Gelatin, Osaka, Japan) in hESF9 medium (Cell Science & Technology Institute, Sendai, Japan). The results show that there is a difference between hES/iPS cell lines in attachment activity to type I collagen. This result suggests that there is a difference among cell lines in integrin signaling (Fig. 1).

Based on these findings, we have modified the culture protocol and tried to culture KhES-1 and KhES-3 cell lines on fibronectin (Sigma, St. Louis, MO) in hESF9 medium without feeders (Fig. 2). Matrigel, a basement membrane preparation from the Engelbreth–Holm–Swarm mouse tumor, is often used for feeder-free culture for hES/iPS cells with MEF-conditioned medium (Draper et al. 2004). However, it contains a complex and ill-defined mixture of fibronectin, laminin, type IV collagen, entactin, and heparan sulfate proteoglycans, and various growth factors such as FGF-2, EGF, PDGF, and NGF (Yang et al. 2003). Ludwig et al. (2006) have reported that in place of matrigel, a combination of collagen IV, fibronectin, laminin, and vitronectin supported robust, long-term proliferation of human ES cells in their chemically defined medium TeSR1. We have previously reported by using defined serum-free culture conditions for mouse embryonic stem (mES) cell that integrins regulate mES cell self-renewal. mES cells remained undifferentiated when cultured on type I and type IV collagen or poly-D-lysine whereas they differentiated when cultured on laminin or fibronectin where LIF-induced self-renewal signaling was decreased (Hayashi et al. 2007). Now, we are investigating the role of integrins in the pluripotency of hES/iPS cells.

For robust cultures, we have further modified the culture protocol. We have used 1 U/ml dispase (Roche Applied Science, Indianapolis, IN) to dissociate the cell colonies and washed the dispase with the medium supplemented with recombinant human albumin (1 mg/ml, Millipore, Bedford, MA). If differentiated cells appear in the culture, addition of low concentration of activin (2~10 ng/ml, R&D Systems, Minneapolis, MN) or middle concentration of noggin (10~20 ng/ml, R&D Systems) seems also to inhibit the differentiated cell growth as previously reported (Beattie et al. 2005; James et al. 2005; Vallier et al. 2005; Wang et al. 2005). However, addition of these growth factors confounds the analysis of the actions of other exogenous factors. We are using hESF9 medium to develop a drug screening test.

It would be convenient if the cell culture novice could propagate and passage any type of cell without difficulty. Unfortunately, this is currently not the case for undifferentiated hES/iPS cell lines. Although serum has proved to be a universal medium supplement that allowed the isolation and characterization of a few normal diploid cell lines and numerous abnormal transformed cell lines over the years, the use of serum or other undefined medium components impedes our ability to understand cell responses to controlled environmental stimuli. There are advantages and disadvantages to culturing hES/iPS cells under defined serum-free culture conditions, and the suitability of any particular medium depends on the purpose of the experiment.

Acknowledgments We thank Prof. P.W. Andrews for his valuable comments and discussion. We thank Hiroko Matsumura, Midori Hayashi, and Yutaka Ozawa for excellent assistance. This study was supported by a grant from the Ministry of Health, Labor and Welfare of Japan to M.K.F., by a grant from the Nipro Corp. and Itochu Corp. to M.K.F., by grants-in-aid for Japan Science and Technology Agency to M.K.F., by grants-in-aid for Scientific Research from the Ministry of Education, Culture, Sports, Science and Technology of Japan to M. K.F. and T.O., and by a Short-Term Fellowship from the Japan Society for the Promotion of Science to J.D.S.

References

Adewumi O.; Aflatoonian B.; Ahrlund-Richter L.; Amit M.; Andrews P. W.; Beighton G.; Bello P. A.; Benvenisty N.; Berry L. S.; Bevan S.; Blum B.; Brooking J.; Chen K. G.; Choo A. B.; Churchill G. A.; Corbel M.; Damjanov I.; Draper J. S.; Dvorak P.; Emanuelsson K.; Fleck R. A.; Ford A.; Gertow K.; Gertsenstein M.; Gokhale P. J.; Hamilton R. S.; Hampl A.; Healy L. E.; Hovatta O.; Hyllner J.; Imreh M. P.; Itskovitz-Eldor J.; Jackson J.; Johnson J. L.; Jones M.; Kee K.; King B. L.; Knowles B. B.; Lako M.; Lebrin F.; Mallon B. S.; Manning D.; Mayshar Y.; McKay R. D.; Michalska A. E.; Mikkola M.; Mileikovsky M.; Minger S. L.; Moore H. D.; Mummery C. L.; Nagy A.; Nakatsuji N.; O'Brien M.; Oh C. S. K.; Olsson C.;

Otonkoski T.; Park K. Y.; Passier R.; Patel H.; Patel M.; Pedersen R.; Pera M. F.; Piekarczyk M. S.; Pera R. A.; Reubinoff B. E.; Robins A. J.; Rossant J.; Rugg-Gunn P.; Schulz T. C.; Semb H.; Sherrer E. S.; Siemen H.; Stacey G. N.; Stojkovic M.; Suemori H.; Szatkiewicz J.; Turetsky T.; Tuuri T.; van den Brink S.; Vintersten K.; Vuoristo S.; Ward D.; Weaver T. A.; Young L. A.; Zhang W. Characterization of human embryonic stem cell lines by the International Stem Cell Initiative. *Nat. Biotechnol.* 25: 803–816; 2007.

Amit M.; Carpenter M. K.; Inokuma M. S.; Chiu C. P.; Harris C. P.; Waknitz M. A.; Itskovitz-Eldor J.; Thomson J. A. Clonally derived human embryonic stem cell lines maintain pluripotency and proliferative potential for prolonged periods of culture. *Dev. Biol.* 227(2): 271–278; 2000.

Barnes D.; Sato G. Serum-free cell culture: a unifying approach. *Cell* 22: 649–655; 1980.

Beattie G. M.; Lopez A. D.; Bucay N.; Hinton A.; Firpo M. T.; King C. C.; Hayek A. Activin A maintains pluripotency of human embryonic stem cells in the absence of feeder layers. *Stem Cells* 23: 489–495; 2005.

Bottenstein J. E.; Sato G. H. Growth of a rat neuroblastoma cell line in serum-free supplemented medium. *Proc. Natl. Acad. Sci. USA* 76: 514–517; 1979.

Draper J. S.; Moore H. D.; Ruban L. N.; Gokhale P. J.; Andrews P. W. Culture and characterization of human embryonic stem cells. *Stem Cells Dev.* 13: 325–336; 2004.

Fassler, R.; Meyer, M. W. Consequences of lack of beta 1 integrin gene expression in mice. *Genes Dev.* 9: 1896–1908; 1995.

Furue M.; Okamoto T.; Ikeda M.; Tanaka Y.; Sasaki Y.; Nishihira K.; Sato J. D. Primitive neuroectodermal tumor cell lines derived from a metastatic pediatric tumor. *In Vitro Cell Dev. Biol. Anim.* 30A: 813–816; 1994.

Furue M. K.; Na J.; Jackson J. P.; Okamoto T.; Jones M.; Baker D.; Hata R.; Moore H. D.; Sato J. D.; Andrews P. W. Heparin promotes the growth of human embryonic stem cells in a defined serum-free medium. *Proc. Natl. Acad. Sci. USA* 105: 13409–13414; 2008.

Hayashi I.; Sato G. H. Replacement of serum by hormones permits growth of cells in a defined medium. *Nature* 259: 132–134; 1976.

Hayashi Y.; Furue M. K.; Okamoto T.; Ohnuma K.; Myoishi Y.; Fukuhara Y.; Abe T.; Sato J. D.; Hata R.; Asashima M. Integrins regulate mouse embryonic stem cell self-renewal. *Stem Cells* 25: 3005–3015; 2007.

James D.; Levine A. J.; Besser D.; Hemmati-Brivanlou A. TGFbeta/activin/nodal signaling is necessary for the maintenance of pluripotency in human embryonic stem cells. *Development* 132: 1273–1282; 2005.

Ludwig T. E.; Levenstein M. E.; Jones J. M.; Berggren W. T.; Mitchen E. R.; Frane J. L.; Crandall L. J.; Daigh C. A.; Conard K. R.; Piekarczyk M. S.; Llanas R. A.; Thomson J. A. Derivation of human embryonic stem cells in defined conditions. *Nat. Biotechnol.* 24: 185–187; 2006.

Nakatsuji N. Establishment and manipulation of monkey and human embryonic stem cell lines for biomedical research. *Ernst Schering Res. Found. Workshop.* 54: 15–26; 2005.

Okamoto T.; Tani R.; Yabumoto M.; Sakamoto A.; Takada K.; Sato G. H.; Sato J. D. Effects of insulin and transferrin on the generation of lymphokine-activated killer cells in serum-free medium. *J. Immunol. Methods* 195: 7–14; 1996.

Reubinoff B. E.; Pera M. F.; Fong C. Y.; Trounson A.; Bongso A. Embryonic stem cell lines from human blastocysts: somatic differentiation in vitro. *Nat. Biotechnol.* 18: 399–404; 2000.

Sato J. D.; Barnes D.; Hayashi I.; Hayashi J.; Hoshi H.; Kawamoto T.; Matsuda R.; McKeehan W. L.; Matsuzaki K.; Okamoto T.; Serrero G.; Sussman D. J.; Kan M. et al. In: Davis J. M. (ed) Specific cells and their requirements. Basic cell culture: a practical approach. Oxford University Press, Oxford, pp 227–274; 2002.

Sato J. D.; Kawamoto T,.; Okamoto T. Cholesterol requirement of P3-X63-Ag8 and X63-Ag8.653 mouse myeloma cells for growth in vitro. *J. Exp. Med.* 165: 1761–1766; 1987.

Skottman H.; Hovatta O. Culture conditions for human embryonic stem cells. *Reproduction* 132: 691–698; 2006.

Thomson J. A.; Itskovitz-Eldor J.; Shapiro S. S.; Waknitz M. A.; Swiergiel J. J.; Marshall V. S.; Jones J. M. Embryonic stem cell lines derived from human blastocysts. *Science* 282: 1145–1147; 1998.

Vallier L.; Alexander M.; Pedersen R. A. Activin/Nodal and FGF pathways cooperate to maintain pluripotency of human embryonic stem cells. *J. Cell Sci.* 118: 4495–4509; 2005.

Wang G.; Zhang H.; Zhao Y.; Li J.; Cai J.; Wang P.; Meng S.; Feng J.; Miao C.; Ding M.; Li D.; Deng H. Noggin and bFGF cooperate to maintain the pluripotency of human embryonic stem cells in the absence of feeder layers. *Biochem. Biophys. Res. Commun.* 330: 934–942; 2005.

Yang J. Z.; Ho A. L.; Ajonuma L. C.; Lam S. Y.; Tsang L. L.; Tang N.; Rowlands D. K.; Gou Y. L.; Chung Y. W.; Chan H. C. Differential effects of Matrigel and its components on functional activity of CFTR and ENaC in mouse endometrial epithelial cells. *Cell Biol. Int.* 27: 543–548; 2003.

of a prospective randomized trial of the German Low Grade Lymphoma Study Group (GLSG). *Journal of Clinical Oncology*, **23**, 1984–1992.

Orciuolo, E., Buda, G., Cecconi, N., Galimberti, S., Versari, D., Cervetti, G., Salvetti, A. & Petrini, M. (2007) Unexpected cardiotoxicity in haematological bortezomib treated patients. *British Journal of Haematology*, **138**, 396–397.

Orlowski, R.Z., Nagler, A., Sonneveld, P., Blade, J., Hajek, R., Spencer, A., San Miguel, J., Robak, T., Dmoszynska, A., Horvath, N., Spicka, I., Sutherland, H.J., Suvorov, A.N., Zhuang, S.H., Parekh, T., Xiu, L., Yuan, Z., Rackoff, W. & Harousseau, J.L. (2007) Randomized phase III study of pegylated liposomal doxorubicin plus bortezomib compared with bortezomib alone in relapsed or refractory multiple myeloma: combination therapy improves time to progression. *Journal of Clinical Oncology*, **25**, 3892–3901.

Sonneveld, P., Hajek, R., Nagler, A., Spencer, A., Blade, J., Robak, T., Zhuang, S.H., Harousseau, J.L. & Orlowski, R.Z. (2008) Combined pegylated liposomal doxorubicin and bortezomib is highly effective in patients with recurrent or refractory multiple myeloma who received prior thalidomide/lenalidomide therapy. *Cancer*, **112**, 1529–1537.

Keywords: bortezomib, fludarabine, liposomal doxorubicin, mantle cell lymphoma, rituximab.

First published online 16 November 2009
doi: 10.1111/j.1365-2141.2009.07998.x

Serum granulysin as a possible biomarker of natural killer cell neoplasms

Granulysin is a cytolytic and proinflammatory molecule that is excreted from cytotoxic T lymphocytes (CTL) and natural killer (NK) cells. It is synthesized as a 15-kDa molecule and then cleaved at the amino and carboxy termini to produce an active 9-kDa form (Pena *et al*, 1997). Equivalent amounts of these two forms of granulysin are found in CTL and NK cells. However, the 9-kDa form is sequestered in cytolytic granules, while the 15-kDa form is constitutively secreted and more stable than the 9-kDa form when excreted *in vivo*. Therefore, the 15-kDa form constitutes a major portion of serum granulysin (Ogawa *et al*, 2003) and is considered to be a biomarker.

We have previously reported that serum granulysin reflects on cellular immune capacity (Ogawa *et al*, 2003), anti-tumour activity (Nagasawa *et al*, 2005) and graft-*versus*-host reaction in allogeneic transplantation (Nagasawa *et al*, 2006). Recently, it has been reported that granulysin is an important mediator of keratinocyte death in Stevens–Johnson syndrome and toxic epidermal necrolysis (Chung *et al*, 2008). Considering that granulysin is usually expressed in activated CTL, but not in resting or naive CTL, and constitutively expressed in NK cells, it was speculated that serum granulysin could be a biomarker for NK cell-related disease.

In this context, serum granulysin was retrospectively investigated in a patient with long-term NK type chronic active Epstein–Barr virus (EBV) infection (CAEBV). Serum granulysin was measured using our previously reported enzyme-linked immunosorbent assay method (Ogawa *et al*, 2003).

The patient presented with hydroa vacciniforme at the age of 8 years, and was diagnosed as NK type CAEBV when aged 9 years. In addition to the aggravation of facial skin lesion, general malaise progressed gradually. She was referred to our hospital at 16 years of age, and infusion of autologous activated T cells was started as a cell therapy. As no improvement was achieved, cytotoxic chemotherapy was started to eradicate EBV-infected cells. Although EBV load was markedly reduced after chemotherapy, the skin lesion did not improve and biopsy revealed the presence of EBV-infected cells (Fig 1B).

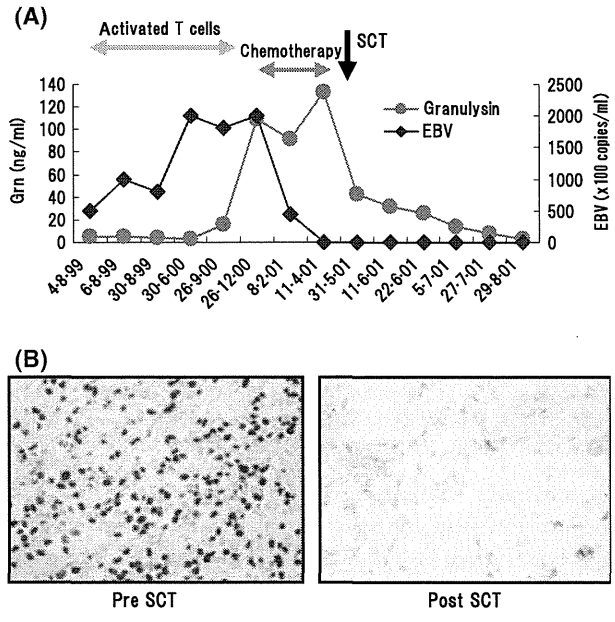

Fig 1. (A) Serum granulysin levels (Grn) and EBV genome load in the peripheral blood in a patient with NK type CAEBV. (B) EBV-infected cells in facial skin disappeared after SCT. EBER positive cells are stained dark brown. Original magnification ×400.

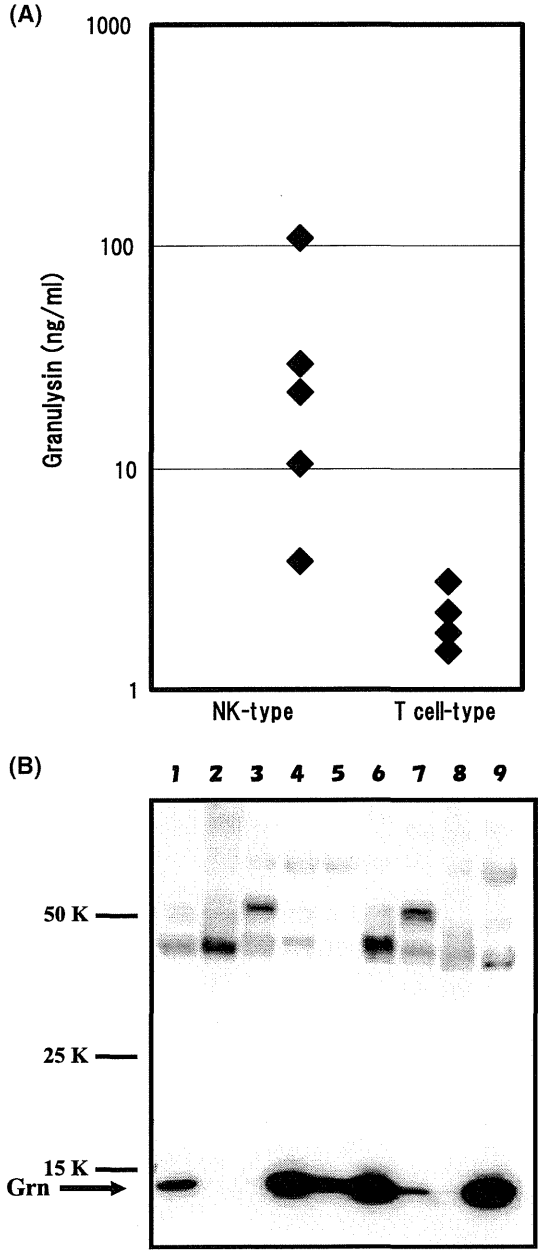

Fig 2. (A) Serum granulysin levels in five NK-type and four T cell-type (αβT) patients with CAEBV. (B) Expression of granulysin in EBV infected NK and γδ T cell lines. The monoclonal antibody, RF10 (Ogawa *et al*, 2003), which reacts with 15-kDa but not 9-kDa granulysin, was used for Western blotting. Lane number and cell line; 1:SNK1(NK) 2:SNK6(NK) 3:SNK8(γδT) 4:SNK10(NK) 5:SNK11(NK) 6:SNK5(NK) 7:SNK15(γδT) 8:SNK16(γδT) 9:SNK20(γδT).

In order to totally cure this condition, the patient received a bone marrow stem cell transplantation (SCT) from a human leucocyte antigen-identical unrelated donor at the age of 18 years. A skin biopsy performed after SCT showed complete disappearance of EBVinfected cells, and serum granulysin was reduced to levels within the normal range (1·5 ± 3·0 ng/ml; Fig 1A) (Ogawa *et al*, 2003).

We also investigated serum granulysin levels in patients with NK type and T cell-type (αβT cell) CAEBV (Kimura *et al*, 2005). Serum granulysin was elevated in NK type but not in T cell-type CAEBV (Fig 2A). Interestingly, serum granulysin was significantly elevated in one patient whose γδ T cells were infected with EBV (data not shown). Next, we investigated the expression of granulysin in several EBV-infected cell lines that were established from CAEBV patients. As expected, most of the NK and γδ T cell lines expressed granulysin (Fig 2B). (SNK11 clone was established from the patient described above and it was clonal in terms of EBV infection). Interestingly, tumour necrosis factor α (TNF-α) was exclusively excreted from the granulysin-expressing cell lines, although interferon-γ was produced in all cell lines (data not shown). From these observations, serum granulysin seems to be a useful biomarker of NK cell neoplasms and could be a marker of its malignant transformation, although the NK proliferative diseases examined here were all EBV-related. Comparison between EBV- and non-EBV- related NK or γδT cell disorders is also an interesting issue regarding not only their pathophysiology but also the mechanism of granulysin regulation, which is not precisely known yet. Further investigation is required to determine its clinical use and significance.

Masayuki Nagasawa[1]
Kazuyuki Ogawa[2]
Kinya Nagata[2]
Norio Shimizu[3]

[1]*Department of Developmental Biology, Tokyo Medical and Dental University, Post Graduate School, Tokyo,* [2]*B.M.L. R&D Centre, Saitama, and* [3]*Department of Virology, Tokyo Medical and Dental University, Post Graduate School, Tokyo, Japan.*
E-mail: mnagasawa.ped@tmd.ac.jp

References

Chung, W.H., Hung, S.I., Yang, J.Y., Su, S.C., Huang, S.P., Wei, C.Y., Chin, S.W., Chiou, C.C., Chu, S.C., Ho, H.C., Yang, C.H., Lu, C.F., Wu, J.Y., Liao, Y.D. & Chen, Y.T. (2008) Granulysin is a key mediator for disseminated keratinocyte death in Stevens–Johnson syndrome and toxic epidermal necrolysis. *Nature Medicine*, **12**, 1343–1350.

Kimura, H., Hoshino, Y., Hara, S., Sugaya, N., Kawada, J., Shibata, Y., Kojima, S., Nagasaka, T., Kuzushima, K. & Morishima, T. (2005) Differences between T cell-type and natural killer cell-type chronic active Epstein–Barr virus infection. *The Journal of Infectious Disease*, **191**, 531–539.

Nagasawa, M., Kawamoto, H., Tsuji, Y. & Mizutani, S. (2005) Transient increase of serum granulysin in stage IVs neuroblastoma patient during spontaneous regression: case report. *International Journal of Hematology*, **82**, 456–457.

Nagasawa, M., Isoda, T., Itoh, S., Kajiwara, M., Morio, T., Shimizu, N., Ogawa, K., Nagata, K., Nakamura, M. & Mizutani, S. (2006) Analysis of serum granulysin in patients with hematopoietic stem cell transplantation: its usefulness as a marker of graft-versus-host reaction. *American Journal of Hematology*, **81**, 340–348.

Ogawa, K., Takamori, Y., Suzuki, K., Nagasawa, M., Takano, S., Kasahara, Y., Nakamura, Y., Kondo, S., Sugamura, K., Nakamura, M. & Nagata, K. (2003) Granulysin in human serum as a marker of cell-mediated immunity. *European Journal of Immunology*, **33,** 1925–1933.

Pena, S.V., Hanson, D.A., Carr, B.A., Goralski, T.J. & Krensky, A.M. (1997) Processing, subcellular localization, and function of 519 (granulysin), a human late T cell activation molecule with homology to small, lytic, granule proteins. *Journal of Immunology*, **158,** 2680–2688.

Keywords: granulysin, natural killer cells, chronic active EBV infection, γδ T cells.

First published online 13 November 2009
doi: 10.1111/j.1365-2141.2009.07999.x

Cancer Science
The official journal of the Japanese Cancer Association JCA

Dominant-negative derivative of EBNA1 represses EBNA1-mediated transforming gene expression during the acute phase of Epstein–Barr virus infection independent of rapid loss of viral genome

Yumi Kariya,[1,2] Makiko Hamatake,[1] Emiko Urano,[1] Hironori Yoshiyama,[3] Norio Shimizu[2] and Jun Komano[1,4]

[1]AIDS Research Center, National Institute of Infectious Diseases, Tokyo; [2]Department of Virology, Division of Medical Science, Medical Research Institute, Tokyo Medical and Dental University, Tokyo; [3]Research Center for Infection-associated Cancer, Institute for Genetic Medicine, Hokkaido University, Sapporo, Japan

(Received November 1, 2009/Revised November 30, 2009/Accepted December 6, 2009/Online publication February 2, 2010)

The oncogenic human herpes virus, the Epstein–Barr virus (EBV), expresses EBNA1 in almost all forms of viral latency. EBNA1 plays a major role in the maintenance of the viral genome and in the transactivation of viral transforming genes, including EBNA2 and latent membrane protein (LMP-1). However, it is unknown whether inhibition of EBNA1 from the onset of EBV infection disrupts the establishment of EBV's latency and transactivation of the viral oncogenes. To address this, we measured EBV infection kinetics in the B cell lines BALL-1 and BJAB, which stably express a dominant-negative EBNA1 (dnE1) fused to green fluorescent protein (GFP). The EBV genome was surprisingly unstable 1 week post-infection: the average loss rate of EBV DNA from GFP- and GFP-dnE1-expressing cells was 53.4% and 41.0% per cell generation, respectively, which was substantially higher than that of an 'established' *oriP* replicon (2–4%). GFP-dnE1 did not accelerate loss of the EBV genome, suggesting that EBNA1-dependent licensing of the EBV genome occurs infrequently during the acute phase of EBV infection. In the subacute phase, establishment of EBV latency was completely blocked in GFP-dnE1-expressing cells. In contrast, C/W promoter-driven transcription was strongly restricted in GFP-dnE1-expressing cells at 2 days post-infection. These data suggest that inhibition of EBNA1 from the onset of EBV infection is effective in blocking the positive feedback loop in the transactivation of viral transforming genes, and in eradicating the EBV genome during the subacute phase. Our results suggest that gene transduction of GFP-dnE1 could be a promising therapeutic and prophylactic approach toward EBV-associated malignancies. (*Cancer Sci* 2010; 101: 876–881)

The Epstein–Barr virus (EBV) is a risk factor in several malignant diseases including Burkitt's lymphoma and nasopharyngeal carcinoma.[1–4] The opportunistic B-cell lymphoma is becoming the major cause of death in AIDS patients in an era of highly active antiretroviral therapy (HAART), and EBV is associated with a significant portion of AIDS lymphoma cases.[5,6] Neither an EBV vaccine, nor specific antiviral agents against EBV are available; thus attention should be paid to the development of therapeutic agents against EBV.

EBV-encoded genes including EBNA1, EBNA2, and latent membrane protein (LMP-1) are potential molecular targets for the treatment of EBV-associated lymphomas because they play central roles in the process of malignant transformation.[7] We are interested in EBNA1 since it contributes to EBV oncogenesis in two ways: it supports the maintenance of the EBV genome in *cis* and enhances expression of viral oncogenes, including EBNA2 and LMP-1, in *trans*.[7–9] EBNA1 exerts its biological functions by binding to its cognate binding sites within the family of repeats (FR) and the dyad symmetry element (DS) located within the origin of replication (oriP) of EBV DNA. EBNA1 interacts with FR to enhance transcription from the viral C/W promoters (C/Wp) and to partition EBV DNA to daughter cells; and with DS to initiate DNA replication.[7–9]

Maintenance of the oriP replicon is stable once EBV latency has been established. The loss rate of established oriP plasmids is estimated at 2–4% per cell generation.[10,11] Interestingly, the loss rate of the oriP replicon is significantly higher in cells transiently transduced with oriP plasmids (>25% per cell generation) than in established cells.[12] In primary B cells, EBV DNA is lost rapidly within 2 days post-infection (~98.9%).[13] However, the loss rate of the EBV genome during a week post-infection in B cells remains to be quantified.

Upon EBV infection, the first viral genes expressed are the transactivators EBNA2 and EBNA-LP transcribed from Wp several hours after infection.[7] EBNA2 binds to the EBNA2-responsive elements and, in cooperation with EBNA-LP, enhances transcription from Cp, which leads to expression of all EBNA proteins, including EBNA1. EBNA1 binding to oriP activates C/Wp to boost viral latent gene expression, including the EBNAs and LMP-1. The viral gene transactivation positive feedback loop is established within a few days post-infection, and EBNA1 is one of the key factors that sustain this feedback loop during the acute phase of EBV infection.[14] In parallel, EBNA1 contributes to the establishment of the EBV genome as a licensed replicon. It may be possible to stop EBV infection by breaking the chain of EBNA1-dependent events and thus the EBV-mediated malignant transformation of infected cells. Previous studies have assessed the therapeutic potential of a dominant-negative derivative of EBNA1 (dnE1) in cells in which EBV latency was already established.[15,16] In this study, we critically assessed whether inhibition of EBNA1 limits the early stage of EBV infection in B cells. We provide evidence that expression of dnE1 strongly blocks the expression of virus-encoded oncogenes in acutely infected cells without accelerating EBV genome loss, and disrupts EBV latency in the subacute phase of EBV infection.

Materials and Methods

Cells. The 293T, EBV-negative Burkitt lymphoma cell line BJAB, EBV-positive Burkitt lymphoma cell line Daudi, EBV-transformed healthy donor-derived B lymphoblastoid cell line (B-LCL), and B acute lymphoblastic leukemia cell line BALL-1

[4]To whom correspondence should be addressed.
E-mail: ajkomano@nih.go.jp

doi: 10.1111/j.1349-7006.2009.01474.x

cells (kindly provided by Dr. Yokota, National Institute of Infectious Diseases, Tokyo, Japan) were maintained in RPMI-1640 medium (Sigma, St. Louis, MA, USA) supplemented with 10% fetal bovine serum (Japan Bioserum, Tokyo, Japan), 50 U/mL penicillin, 50 μg/mL streptomycin (Invitrogen, Tokyo, Japan), and incubated at 37°C in a humidified 5% CO_2 atmosphere.

Plasmids. The following primers were used to amplify dnE1 from p1160[17] by PCR: 5′-ACCGGTCTCGAGCAATTGCCA-CCATGCGGGGTCAGGGTGATGGAGG-3′ and 5′-GGATC-CTCGAGCGGCCGCTCACTCCTGCCCTTCCTCACC-3′. The GFP-dnE1 expression vector (pGD) was constructed by cloning the MfeI-XhoI fragment of the PCR product into the BglII-SalI sites of pEGFP-C1 (Clontech, Palo Alto, CA, USA). The MfeI and BglII sites were blunted with T7 RNA polymerase. The AgeI-BamHI fragment from pGD was cloned into the corresponding restriction sites of pCMMP eGFP[15,18] to generate pCMMP GFP-dnE1. The EBNA1 expression vector p1553, the FR-tk-luciferase reporter p985, and pLuciferase (pCMV-luc) have been described previously.[17–20]

Luciferase assay. The 293T cells, grown in 48-well plates, were co-transfected with the indicated plasmids using Lipofectamine 2000 according to the manufacturer's protocol (Invitrogen, Tokyo, Japan). Cells were replated in 96-well plates in triplicate at 2 h post-transfection. Luciferase activity was measured 48 h after transfection using the Steady-Glo Kit (Promega, Madison, WI, USA).

Murine leukemia virus (MLV) vector infection and cell sorting. MLV vectors were produced as described previously.[18] B cells (1×10^7 cells) were incubated with 2 mL of MLV preparation overnight at 4°C with continuous agitation. GFP-positive cells were collected using a FACS sorter (FACS Vantage; Becton Dickinson, San Jose, CA, USA) at 11 days post-infection.

Western blotting. Western blotting was performed as described previously.[21,22] The following reagents were used: anti-GFP (MsX Green Fluorescent Protein; Chemicon, Temecula, CA, USA) and Envision$^+$ Dual Link System-HRP (Dako, Glostrup, Denmark).

EBV infection and nucleic acid extraction. The EBV B95-8 strain was a generous gift from Dr Fujiwara's group at the National Research Institute for Child and Development (Tokyo, Japan). B cells (1×10^7 cells) were incubated with 100 μL of B95-8 EBV for 1 h at 37°C, and genomic DNA was extracted from half of the infected cells soon after infection (QIAamp DNA Mini Kit; Qiagen, Tokyo, Japan). At 15 h post-infection, half of the cells were washed once with PBS and incubated for 5 min in lysis buffer (10 mM Tris-HCl [pH7.4], 10 mM NaCl, 3 mM $MgCl_2$, and 0.5% NP-40). The nuclear fraction was collected by centrifugation for 5 min at 20.6 K × *g* (Kubota 3740; Kubota, Tokyo, Japan), and high molecular weight DNA was extracted (nuclear DNA). At 2 days post-infection and at later time points, high molecular weight DNA, or total RNA (PureLink Total RNA Blood Purification Kit; Invitrogen) was extracted from 1×10^6 or 3×10^6 cells, respectively, according to the manufacturer's protocol. After EBV infection, 10 μM aciclovir (Kayaku, Tokyo, Japan) was added to the culture medium. The production and infection of the recombinant EBV Akata strain carrying GFP and neomycin resistant genes has been described previously.[23] At 2 days post-infection, cells were plated at a density of 1×10^4 cells per well in a flat-bottomed 96-well plate, and cultured in a medium containing 1 mg/mL G418. The efficiency of EBV latency establishment was evaluated as percentage of wells positive for the emergence of G418-resistant cells at 2 to 3 weeks post-G418 selection.

Quantitative real-time PCR. Real-time PCR was performed as described previously; serial dilutions of positive controls were used as standards.[21] Amplifications were performed using the QuantiTect SYBR Green RT-PCR/PCR Kit (Qiagen), and the following primers: BamHI W repeat, 5′-GCCAGAGG-TAAGTGGACTTT-3′ and 5′-AGAAGCATGTATACTAAGC-CTCCC-3′; cyclophilin A (CYPA), 5′-CACCGCCACCATG-GTCAACCCCA-3′ and 5′-CCCGGGCCTCGAGCTTTCGAG-TTGTCCACAGTCAGCAATGG-3′; C/Wp, 5′-CCCTCGGA-CAGCTCCTAAG-3′ and 5′-CTTCACTTCGGTCTCCCCTA-3′; EBER1, 5′-AAAACATGCGGACCACCAGC-3′ and 5′-AG-GACCTACGCTGCCCTAGA-3′. The β-globin primers were described previously.[21] Following PCR amplification, the amplicons were separated in a 2% agarose gel, stained with ethidium bromide, and imaged with a Typhoon scanner (GE Healthcare Bio-Sciences; Piscataway, NJ, USA).

Results

Construction and functional verification of dnE1 fused to GFP. The carboxy half of EBNA1 serves as a functional dominant-negative inhibitor of EBNA1 that restricts the replication and maintenance of oriP plasmids as well as the EBNA1-dependent enhancement of transcription.[17,24] We used a dnE1 mutant encompassing amino acids 377 to 391 (the nuclear localization signal, NLS) and 451 to 641 (the DNA binding and dimerization domain) of EBNA1 (Fig. 1A).[17] To visualize the intracellular distribution of dnE1, we constructed the retroviral expression vector encoding GFP-dnE1. The expression of GFP-dnE1 was verified in transiently transfected 293T cells and stably transduced B cell lines using an MLV vector. To verify the function of GFP-dnE1, we conducted a reporter assay using a plasmid encoding the FR-tk-luciferase cassette. EBNA1 enhances expression of FR-tk-luciferase by binding to FR. If the GFP-dnE1 construct retains dnE1 function, co-expressing EBNA1 and GFP-dnE1 should reduce reporter activity. Luciferase activity was increased significantly upon EBNA1 expression by approximately 5.3-fold, consistent with previous findings (Fig. 1B, $P < 0.05$, two-tailed Student's *t*-test).[17] When GFP-dnE1 was co-expressed, the luciferase activity was decreased. The decrease in luciferase activity was proportional to the increase in GFP-dnE1 expression vector (Fig. 1B, maximum reduction: 22.3%, $P < 0.05$, two-tailed Student's *t*-test). This effect was not observed with GFP alone. In addition, CMV promoter-driven luciferase expression was unaffected by EBNA1, GFP-dnE1, and GFP, suggesting that the reduction in luciferase activity with GFP-dnE1 in the EBNA1/FR-tk-luciferase system is specific. These data indicate that GFP-dnE1 functions as an inhibitor of EBNA1.

Establishment of B cells constitutively expressing GFP-dnE1. To investigate the potential effect of GFP-dnE1 on EBV infection in B cells, we established BALL-1 and BJAB cells, which constitutively express GFP-dnE1, using an MLV vector. GFP was used as a control throughout this study. The distribution of GFP-dnE1 was examined by confocal microscopy, which revealed an even distribution of GFP throughout the cell. In contrast, the majority of GFP-dnE1was localized to the nucleus due to the presence of the NLS (Fig. 2A). Similar observations were made in BJAB and 293T cells (data not shown). We sorted the GFP- or GFP-dnE-expressing cells using a FACS sorter. To test the dose-dependent effect, we collected BALL-1 cell populations bearing high or low levels of GFP fluorescence, denoted as Hi and Lo, respectively. The expression of GFP and GFP-dnE1 was verified by Western blotting, which confirmed that GFP and GFP-dnE1 Hi cells had higher intensity signals than the GFP and GFP-dnE1 Lo cells (Fig. 2B). The rate of cell proliferation and the morphology of GFP-dnE1 cells were indistinguishable from those of GFP cells (Fig. 2A and data not shown).

Effect of GFP-dnE1 on the nuclear translocation of EBV DNA during the acute phase of EBV infection. To assess whether GFP-dnE1 could restrict the nuclear targeting of the EBV

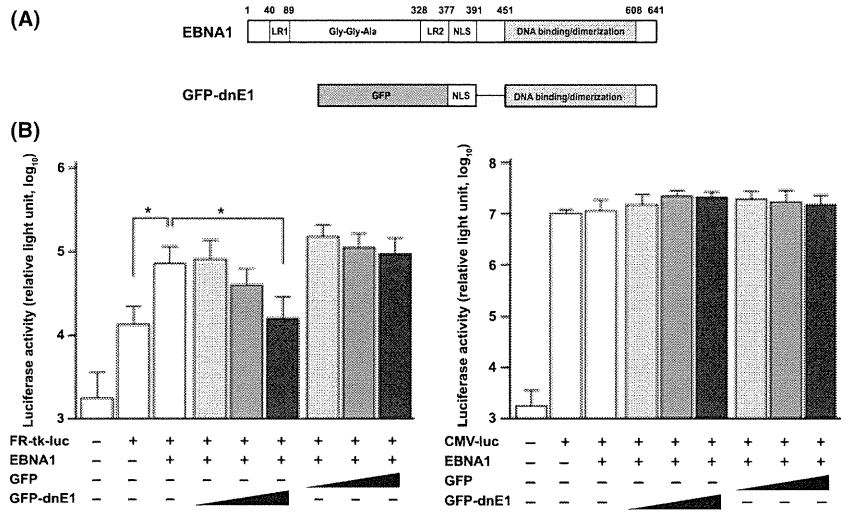

Fig. 1. Construction and functional characterization of a dominant-negative EBNA1 mutant (dnE1) fused to green fluorescent protein (GFP). (A) Structure of the EBNA1 protein and dnE1 used in this study. The linking regions (LR1 and LR2), the Gly-Gly-Ala repeat, the nuclear localization signal (NLS), and the DNA binding and dimerization domain are shown. GFP-dnE1 encodes the NLS and DNA binding and dimerization domain of EBNA1 fused to the C-terminus of GFP. (B) Repression of EBNA1-dependent transcriptional activation by GFP-dnE1. We transfected 293T cells in 48-well plates with 200 ng of FR-tk-luc or CMV-luc reporter, and 500 ng of EBNA1 expression vector, along with increasing amounts of GFP or GFP-dnE1 expression vector (20, 100, and 500 ng, respectively). $*P < 0.05$, two-tailed Student's *t*-test.

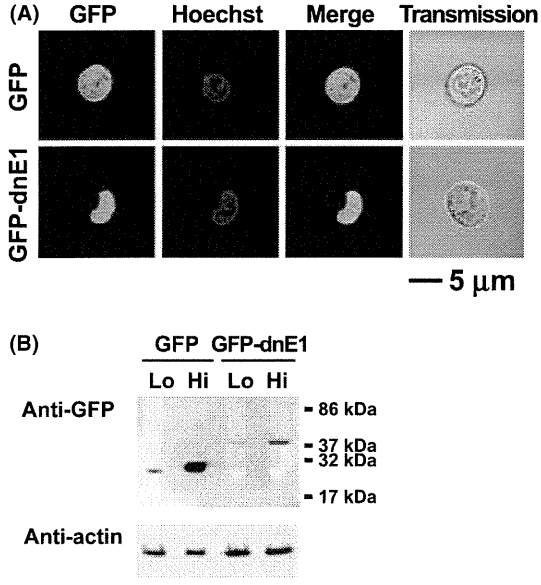

Fig. 2. Verification of stable green fluorescent protein (GFP)-dominant-negative EBNA1 (dnE1) expression in BALL-1 cells. (A) Distribution of GFP and GFP-dnE1 in BALL-1 cells was examined by confocal microscopy. Cells were imaged unfixed using a confocal microscope META 510 (Carl Zeiss, Tokyo, Japan). The green signal represents GFP fluorescence, and blue represents the Hoechst-stained nucleus. The bar represents 5 μm; magnification, ×630. (B) GFP or GFP-dnE1 expression in stably transduced BALL-1 cells was examined by Western blot analysis using an anti-GFP antibody. Protein lysates from 5×10^5 cells were loaded for each sample, except GFP Hi cells (5×10^4). The molecular weight marker is shown on the right.

genome after infection, we measured the amount of EBV DNA recovered from cells immediately after infection (representing the amount of EBV attached to cells) and the amount of EBV DNA that had migrated into the nucleus at 1 day post-infection. We isolated the nuclear fraction to exclude EBV DNA that failed to enter the nucleus. The number of EBV DNA molecules per cell was estimated by real-time PCR, which targeted the BamHI W repeat, in 10 ng of genomic DNA. We estimated the number of EBV DNA per cell given that a single cell contains approximately 10 pg of genomic DNA, and an EBV DNA has 10 copies of BamHI W repeats on average. The nuclear targeting efficiencies of EBV DNA were as follows: BALL-1 GFP cells, 43.3–108.6%; GFP-dnE1 cells, 46.9–65.6%; BJAB GFP cells, 37.4%; GFP-dnE1 cells, 35.0% (Table 1). These data suggested that the effect of GFP-dnE1 on the nuclear targeting of EBV DNA should be assessed more sensitively in BALL-1 and BJAB cell systems than in primary B cells because the nuclear targeting efficiency of EBV DNA in primary B cells is extremely inefficient (~1.1%).[13] In our experimental systems, the nuclear targeting efficiencies of EBV DNA in GFP-dnE1-expressing cells were similar to those in GFP-expressing cells. In addition, the dose-dependency of GFP-dnE1 was not observed in BALL-1 cells (Table 1). These data suggest that the nuclear targeting efficiency of EBV DNA was not restricted by the presence of GFP-dnE1 in B cells upon EBV infection.

Effect of GFP-dnE1 on the rate of loss of EBV DNA during the acute phase of EBV infection. To examine the effect of GFP-dnE1 on the rate of loss (ROL) of EBV DNA during the acute phase of viral infection, we monitored the EBV DNA copy number from day 2 to day 5 or day 6 post-infection, by real-time PCR, which detects the viral genome in both linear and circular configurations (Table 1). The ROL was estimated as the percentage reduction of EBV DNA per cell generation, considering that the cell doubling time is 24 h, and the kinetics of viral genome loss follows an exponential decay. The ROL in GFP-dnE1-expressing cells (19.2–85.9% per cell generation) was similar to GFP-expressing cells (20.5–79.4% per cell generation) in both BALL-1 and BJAB cells. In addition, there was no detectable dose-dependent effect of GFP-dnE1 in BALL-1 cells (Table 1 and Fig. 3). The averages ± SEs of ROL in GFP- and GFP-dnE1-expressing cells from six independent measurements in BALL-1 cells were 37.7 ± 10.7% and 25.7 ± 6.5% per cell generation, respectively (data not shown), which was substantially higher than the rate of loss of an established oriP replicon (2–4%).[10,11] These results reflect the precipitous loss of oriP plas-

doi: 10.1111/j.1349-7006.2009.01474.x

Table 1. The kinetics of EBV DNA in the acute phase of EBV infection

Cell	Copy number of EBV DNA per cell at the indicated day†				Nuclear transport (%‡)	Rate of loss of EBV DNA (% per cell generation§)
Expt 1						
BALL-1	Day 0	Day 1	Day 2	Day 5		
GFP Hi	20.38	11.92	3.57	0.01¶	58.5	85.9
GFP Lo	17.26	11.68	3.21	0.56	67.7	44.1
GFP-dnE1 Hi	23.02	10.79	3.30	0.30	46.9	54.9
GFP-dnE1 Lo	18.83	12.36	1.46	0.53	65.6	28.7
BJAB	Day 0	Day 1	Day 2	Day 5		
GFP	155.1	58.8	5.38	0.06	37.4	77.7
GFP-dnE1	64.6	37.4	5.69	0.05	58.0	79.4
Expt 2						
BALL-1	Day 0	Day 1	Day 2	Day 6		
GFP Hi	16.33	17.73	11.10	4.74	108.6	19.2
GFP Lo	17.35	7.51	8.75	1.13	43.3	40.1
GFP-dnE1 Hi	18.46	8.71	8.95	3.38	47.2	21.6
GFP-dnE1 Lo	14.14	7.05	6.97	2.79	49.9	20.5

†Nuclear DNA was used for day 1 data. ‡Estimated from day 0 and day 1 data. §Estimated from day 2 and day 5 or day 6 data with the exponential decay. ¶Below the limit of detection. dnE1, dominant-negative EBNA1; EBV, Epstein–Barr virus; GFP, green fluorescent protein.

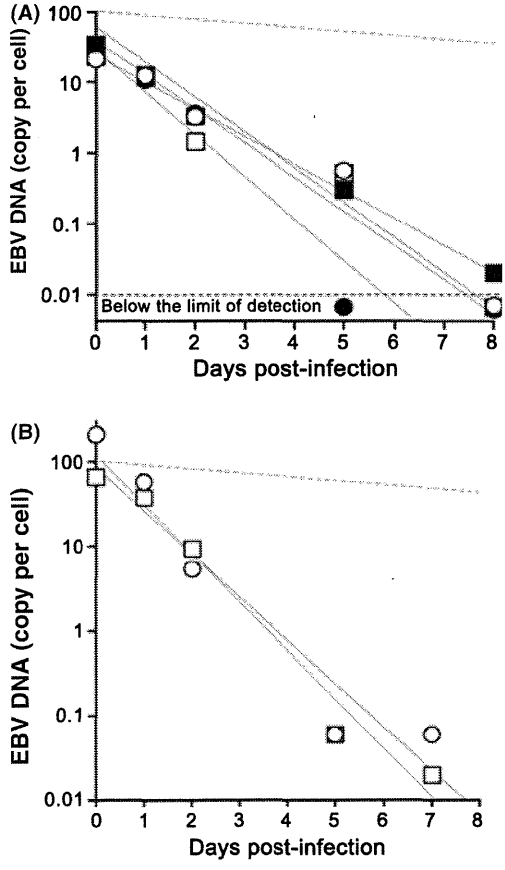

Fig. 3. Kinetics of Epstein–Barr virus (EBV) DNA loss during the acute phase of EBV infection. (A) Representative data from BALL-1 cells (Expt. 1 in Table 1) is shown. The filled squares, open squares, filled circles, and open circles represent GFP Hi, GFP Lo, GFP-dnE1 Hi, and GFP-dnE1 Lo, respectively. The limit of detection was below 0.01 (dashed line). The gray lines represent an approximation to the exponential decay. The dashed gray line represents the 4% rate of loss per cell generation. (B) Representative data from BJAB cells shown in Table 1. The circles and squares represent GFP and GFP-dnE1, respectively. Please see Table 1 for the detailed analysis.

mids (26–37%) in transiently transfected non-B cells.[12] The data suggest that GFP-dnE1 is unable to accelerate the ROL in the acute phase of EBV infection in B cells, presumably because the EBV genome is not established as an EBNA1-dependent stable licensed replicon. It should be noted that this is the first time that quantitative ROL data has been obtained by introducing the oriP replicon into B cells via EBV infection, which is an approach that does not confer any selective advantage on the infected cells.

Effect of GFP-dnE1 on efficiency of establishment of EBV latency. Cells infected with recombinant EBV, carrying the neomycin resistance gene, were seeded at 5×10^3 cells per well into a 96-well plate, and the efficiency of the establishment of EBV latency was assessed as the percentage of wells positive for the emergence of G418-resistant cells. G418-resistant cells appeared in BJAB, Daudi, parental BALL-1, and BALL-1 GFP cells at 56–100% efficiencies. In sharp contrast, G418-resistant cells were absent from GFP-dnE1-expressing BALL-1 cells (Table 2). These data clearly suggest that, although the ROL during the acute phase of EBV infection was not enhanced by GFP-dnE1, GFP-dnE1 was able to block the establishment of EBV latency completely during the subacute phase of EBV infection.

Effect of GFP-dnE1 on EBV-encoded latent gene expression. EBV gene expression was tested at 2 days post-infection by quantitative RT-PCR. We focused on the C/Wp activity because it expresses key viral transactivators including EBNA1, -2, -3s, and -LP to boost viral transforming gene expression. We detected C/Wp-driven transcripts in GFP Hi BALL-1 cells as expected. Conversely, C/Wp-driven transcripts were undetectable in GFP-dnE1 Hi and Lo BALL-1 cells, although these cells retained similar EBV DNA levels to GFP-expressing cells (Fig. 4 and Table 3). The Cp-driven transcript was under the limit of detection by RT-PCR, suggesting that the Wp is predominantly activated at the early phase of EBV infection consistent with previous findings.[7] Inhibition of viral gene transcription was not observed in the RNA polymerase III-driven transcript EBER1,[25] and cyclophilin A mRNA levels were similar between GFP- and GFP-dnE1-expressing cells (Fig. 4 and Table 3). This indicates that the effect of GFP-dnE1 on C/Wp activity is specific, and uncovers an active role of EBNA1 in supporting transactiva-